Plant, Cell and Environment (2003) **26**, 1097–1116

A coupled model of stomatal conductance, photosynthesis and transpiration

A. TUZET[1], A. PERRIER[1] & R. LEUNING[2]

[1]*Environnement et Grandes Cultures INRA – INA PG 78850 Thiverval Grignon, France and* [2]*CSIRO Land and Water, FC Pye Laboratory, Canberra, ACT 2601, Australia*

ABSTRACT

A model that couples stomatal conductance, photosynthesis, leaf energy balance and transport of water through the soil–plant–atmosphere continuum is presented. Stomatal conductance in the model depends on light, temperature and intercellular CO_2 concentration via photosynthesis and on leaf water potential, which in turn is a function of soil water potential, the rate of water flow through the soil and plant, and on xylem hydraulic resistance. Water transport from soil to roots is simulated through solution of Richards' equation. The model captures the observed hysteresis in diurnal variations in stomatal conductance, assimilation rate and transpiration for plant canopies. Hysteresis arises because atmospheric demand for water from the leaves typically peaks in mid-afternoon and because of uneven distribution of soil matric potentials with distance from the roots. Potentials at the root surfaces are lower than in the bulk soil, and once soil water supply starts to limit transpiration, root potentials are substantially less negative in the morning than in the afternoon. This leads to higher stomatal conductances, CO_2 assimilation and transpiration in the morning compared to later in the day. Stomatal conductance is sensitive to soil and plant hydraulic properties and to root length density only after approximately 10 d of soil drying, when supply of water by the soil to the roots becomes limiting. High atmospheric demand causes transpiration rates, LE, to decline at a slightly higher soil water content, θ_s, than at low atmospheric demand, but all curves of LE versus θ_s fall on the same line when soil water supply limits transpiration. Stomatal conductance cannot be modelled in isolation, but must be fully coupled with models of photosynthesis/respiration and the transport of water from soil, through roots, stems and leaves to the atmosphere.

Key-words: photosynthesis; plant canopy modelling; root water absorption; stomatal conductance; transpiration.

Correspondence: Andrée Tuzet. Fax: 33 1 30 81 55 63; e-mail: tuzet@grignon.inra.fr

INTRODUCTION

Although the response of stomata to environmental and physiological factors is complex, we know that stomatal conductance varies with leaf irradiance, leaf temperature, atmospheric water vapour pressure deficit and CO_2 concentration (Cowan 1977; Buckley & Mott 2002). We know additionally that stomatal conductance depends on guard cell and epidermal turgor (Wu, Sharpe & Spence 1985; Comstock & Mencuccini 1998; Mencuccini, Mambelli & Comstock 2000; Franks *et al*. 2001), and that regulation of turgor in these cells requires metabolic energy (Farquhar & Wong 1984; Assman 1999; Blatt 2000; Netting 2000). Leaf turgor also depends on the balance between loss of water through transpiration and supply of water to the leaf from the soil (Cowan 1977; Mott & Parkhurst 1991; Maier-Maercker 1999; Mott & Franks 2001). A major challenge is to develop a model which accounts for all the factors which control stomatal conductance.

There are presently few, if any, models which combine our mechanistic understanding of stomatal function at the cellular level with descriptions of the coupled fluxes water and CO_2 in the soil–plant–atmosphere continuum (SPAC). Instead, the dependencies of stomatal conductance on environmental and physiological factors are included in semi-empirical models, such as the response-function approach of Jarvis (1976), which relates stomatal conductance to leaf temperature, irradiance and leaf and soil water potentials. More recently, Ball, Woodrow & Berry (1987) and Leuning (1990, 1995) developed relationships between stomatal conductance, CO_2 assimilation rate and air humidity which summarized successfully the results of many observations of the stomatal behaviour of well-watered plants. Such models have concentrated on leaf-level process, but to account for the various environmental and physiological controls of stomatal conductance, models of photosynthesis, respiration, leaf energy balances and the transport of water from soil to leaves should be fully integrated with stomatal models.

This continuum approach has been adopted by many workers, but there are marked differences in the way stomatal control of water and CO_2 fluxes have been modelled. Some emphasize plant physiology (e.g. Leuning *et al*. 1995) whereas others provide a greater balance between soil,

plant and atmospheric processes affecting carbon and water fluxes (e.g. Sellers *et al*. 1992; McMurtrie *et al*. 1992; Jensen *et al*. 1993; Tardieu & Davies 1993; Williams *et al*. 1996; Baldocchi & Meyers 1998; Whitehead *et al*. 2002; Dewar 2002). Many such models are satisfactory when soil moisture is adequate, but some do not predict correctly the patterns in conductance, transpiration and CO_2 assimilation when soil moisture availability becomes limiting (e.g. Calvet *et al*. 1998; Grant *et al*. 1999). Measured fluxes show a marked daytime asymmetry at low soil moisture contents, with higher fluxes of water and CO_2 in the morning than the afternoon (Schulze & Hall 1982; Olioso, Carlson & Brisson 1996; Prior, Eamus & Duff 1997; Grant *et al*. 1999; Eamus, Hutley & O'Grady 2001). Whereas some models are able to capture the observed asymmetry (Tardieu & Davies 1993), those of others are not (Leuning *et al*. 1995; Leuning, Dunin & Wang 1998; Grant *et al*. 1999; Ronda, de Bruin & Holtslag 2001), and we suggest this may result from inadequate coupling of stomatal conductance to the dynamics of water transport from soil to the roots and leaves. Many SPAC models which do incorporate the effects of soil moisture on stomatal conductance use an electrical resistance analog for the transport of water from the soil to the roots (Tardieu & Davies 1993; Amthor 1994; Olioso *et al*. 1996; Williams *et al*. 1996; Baldocchi & Meyers 1998). Hydraulic resistance to water flow in the soil varies strongly with soil moisture. Cowan (1965) showed that water content, and hence hydraulic resistance, varies significantly with distance from the root surface to the bulk soil once soil water supply starts to limit transpiration. Thus use of mean soil moisture content, rather than the value near to the roots, may lead to incorrect values for the resistance to water flow in the soil. The spatial distribution in moisture content also changes through the day and hence the dynamics of water flow to the roots will not be captured when mean soil moisture content is used to calculate soil hydraulic resistance (Perrier & Tuzet 1998). To overcome this problem, the model presented in this paper solves Richards' equation for water flow from the soil to roots numerically (Philip 1957; Gardner 1960), rather than using hydraulic resistances.

Water potentials within the leaf are linked to potentials at the soil–root interface by the flux of water across hydraulic resistances in the plant. We assume that leaf water potential controls stomatal conductance (Buckley & Mott 2002; Leuning, Tuzet & Perrier 2003), an assumption that accounts for the effects of supply and demand for water at the evaporating sites on guard cell and epidermal turgor. This removes the explicit dependence of stomatal conductance on atmospheric humidity used by Ball *et al*. (1987) and by Leuning (1990, 1995), since their models account only for water losses from the leaves by transpiration.

Supply and demand for CO_2 by photosynthesis and respiration also affects stomatal conductance through variations in intercellular CO_2 concentration (Mott 1988; Assmann 1999). These considerations, along with the above arguments concerning leaf water potentials, have led in this paper to a revision of the stomatal model of Leuning (1995). While retaining the explicit dependence of conductance on CO_2 assimilation (and hence on absorbed light and temperature), the original humidity deficit term is replaced by a function of leaf water potential, and CO_2 concentration at the leaf surface is replaced by intercellular CO_2 concentration. This approach ensures a complete coupling between stomatal conductance, the flux of water through the plant and soil, and CO_2 exchange between leaves and the atmosphere.

In the following two sections we briefly describe the new stomatal model and the equations for uptake of water by roots and transport of water through the plants. Appendix A contains details of the rest of the model which describes exchanges of radiant energy, sensible heat, water vapour and CO_2 between the soil, plant and the atmosphere. After presenting the initial and boundary conditions, the full model is used to predict diurnal patterns of leaf water potential, water absorption by roots, and canopy transpiration during a drying cycle for soils with varying hydraulic characteristics. Sensitivity of the model to variations in key controlling parameters is investigated, followed by an examination of the relationships between stomatal conductance, CO_2 assimilation, transpiration, intercellular CO_2 concentrations and atmospheric humidity deficit.

MODEL DESCRIPTION

Stomatal conductance

Several studies have used various forms of the Ball–Berry model for stomatal conductance (Ball *et al*. 1987; Collatz *et al*. 1991; Sellers *et al*. 1992; Leuning 1995; Leuning *et al*. 1995). Although this model is satisfactory for describing the gas exchange of well-watered plants, it is inadequate for plants subjected to some degree of water stress. Wang & Leuning (1998) modified the stomatal model of Leuning (1995) to account for slow changes in soil water content, but that function cannot describe the diurnal response of stomata to the competing demand of water vapour from the atmosphere and supply of water to leaves by the soil via the roots and xylem. To overcome this deficiency, we propose a variant of Leuning's (1995) model which incorporates stomatal response to leaf water potential, namely:

$$g_{co2} = g_0 + \frac{aA}{c_i - \Gamma} \cdot f_{\psi v} \qquad (1)$$

where g_{CO2} is stomatal conductance for CO_2, g_0 is the residual conductance (limiting value of g_{CO2} at the light compensation point), A is assimilation rate, c_i is CO_2 concentration in the intercellular spaces, Γ is the CO_2 compensation point, and a is an empirical coefficient. (see Appendix d for a full list of symbols). The use of c_i in Eqn 1, rather than CO_2 concentration at the leaf surface, c_s (Ball *et al*. 1987; Leuning 1995), agrees with observations that stomata respond to substomatal CO_2 concentration, c_i (Mott 1988; Assmann 1999). Dewar (2002) also used c_i in his model.

An empirical logistic function is used to describe the sensitivity of stomata to leaf water potential:

$$f_{\psi v} = \frac{1+\exp[s_f\psi_f]}{1+\exp[s_f(\psi_f-\psi_v)]} \quad (2)$$

where ψ_v is the bulk leaf water potential, ψ_f is a reference potential and s_f is a sensitivity parameter. With this function we assume that stomata are insensitive to leaf water potential at values close to zero and that stomata rapidly close with decreasing ψ_v (see Fig. 6a). The value of the parameters s_f and ψ_f depend on morphological adaptations in different species (Schulze & Hall 1982; Henson, Jensen & Turner 1989; Sperry 2000) and with environmental conditions experienced during growth (e.g. Saliendra, Sperry & Comstock 1995). Inclusion of leaf water potential in the stomatal model is consistent with the hypothesis of Tyree & Sperry (1988), Jones & Sutherland (1991), and Sperry (2000) who argue that stomata regulate transpiration rates to avoid cavitation in the xylem, and with Buckley & Mott (2002) who postulate that water potential at the evaporating sites within the leaf controls stomatal conductance. Maier-Maercker (1998), Bond & Kavanagh (1999) and Leuning *et al*. (2003) provide further support for this approach to modelling interactions between leaf water potential and stomatal conductance.

Water uptake by roots and transport through the canopy

Cylindrical geometry and the concept of effective soil volume per unit root length have been used to model uptake of water by roots (Philip 1957; Gardner 1960). The roots are taken to be long cylinders with uniform radius and water-absorbing properties, and water movement in the soil is assumed to occur only in the radial direction. The absorbing roots are assumed to be uniformly distributed throughout the entire soil volume. Under these conditions, Richards' flow equation is then:

$$\frac{\partial\theta_s}{\partial t} = \frac{1}{r}\frac{\partial}{\partial r}\left(rK_s\frac{\partial\psi_s}{\partial r}\right) \quad (3a)$$

where θ_s is the soil water content; t is time; r is radial distance from the axis of the root; K_s is soil hydraulic conductivity and Ψ_s is soil water potential. Using the 'Kirchhoff transform', an integral transform that uses a 'matric flux potential', $\phi_s = \int_{-\infty}^{\psi_s} K_s(\psi)\,d\psi$ as a driving force for flow, Equation 3a becomes:

$$\frac{\partial\theta_s}{\partial t} = \frac{1}{r}\frac{\partial}{\partial r}\left(r\,\frac{\partial\phi_s}{\partial r}\right) \quad (3b)$$

Both Ψ_s and K_s depend on soil water content θ_s according to the empirical relationships (Campbell 1985):

$$\psi_s = \psi_e\cdot(\theta_{sat}/\theta_s)^b \quad (4a)$$

$$K_s = K_{sat}\cdot\left(\frac{\theta_s}{\theta_{sat}}\right)^{2b+3} \quad (4b)$$

Table 1. Parameter values to describe soil hydraulic properties using Eqn 4

Type	b	θ_{sat} ($m^3\ m^{-3}$)	ψ_e (MPa)	K_{sat} ($s^{-1}\ MPa^{-1}\ m^2$)
Sandy loam	3.31	0.4	-0.91×10^{-3}	957.6×10^{-6}
Silt loam	4.38	0.4	-1.58×10^{-3}	217.8×10^{-6}
Loam	6.58	0.4	-1.88×10^{-3}	228.6×10^{-6}

where ψ_e is the air entry water potential of the soil, θ_{sat} is the saturation water content, K_{sat} is the saturated conductivity and b is an empirical parameter. Calculations in this paper are based upon data for three soils: sandy loam, silt loam and loam, and values of ψ_e, K_{sat}, θ_{sat} and b for these soils are listed in Table 1. Initial water content is assumed to be uniform throughout the soil volume with some value θ_0, corresponding to a soil water potential ψ_0. The radial flow of water is set to zero at the half average distance between neighbouring roots.

Water uptake by the roots is assumed equal to the flow of water through the plant canopy, F, given by:

$$F = \frac{\psi_r-\psi_v}{\chi_v} = \frac{M_v}{R\rho_v}\frac{1}{r_{sH2O}+r_{bV}}\left(\frac{h_i P(T_{sv})}{T_{sv}}-\frac{P(T_{rv})}{T_{av}}\right) \quad (5)$$

where ψ_r is the water potential at the boundary between the plant roots and the soil and χ_v is the leaf-specific resistance to water flow through plant from the roots to the stomata. Reid & Huck (1990) and Sperry (2000) found that χ_v is correlated to flow rate, but their findings could result from uncertainties in the determining ψ_r experimentally. In practice it is extremely difficult to separate plant and soil resistances to water flow because the latter depends on microgradients around the root zone. Thus χ_v is taken as constant in our calculations.

The second part of Eqn 5 equates the steady-state flow of water through the plant with transpiration; $r_{sH2O} = \beta/(1.6g_{CO2})$ and r_{bv} are the resistances to water transport through the stomata and boundary layer, respectively. The factor 1.6 accounts for the ratio of molecular diffusivities for water and CO_2 in air and β (= P/RT) is the coefficient used to convert the molar units ($mol^{-1}\ m^2\ s$) into physical resistance units ($s\ m^{-1}$) and P is the atmospheric pressure, M_v is the molecular mass of water, R is the ideal gas constant, ρ_v is the liquid water density, $h_i = \exp(M_v\psi_v/\rho_v RT_{sv})$ is the fractional relative humidity in the intercellular spaces. This expression links the thermodynamic potential of water in the liquid and gas phases at the evaporating sites within the leaf. The functions $P(T_{sv})$ and $P(T_{rv})$ are the saturation water vapour pressure at foliage temperature T_{sv} and dew-point temperature of the air surrounding leaves T_{rv}, while T_{av} is air temperature.

System modelled

The full model framework is shown in Fig. 1. Fluxes, water contents, and associated quantities are expressed on the

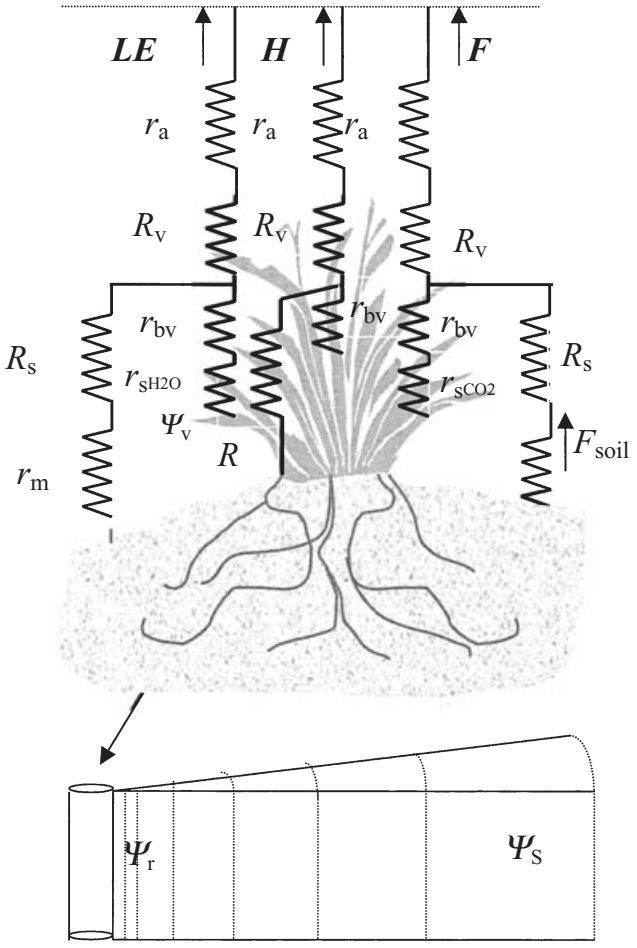

Figure 1. Schematic diagram of the latent heat, sensible heat and CO_2 exchange system described by the model. The cylindrical geometry used to calculate the flow of water to the root is also shown.

basis of unit area of ground, the plant is divided into shoots and roots and there is only one soil layer. Although the model is relatively simple, its main purpose is to demonstrate the intimate connection between stomatal conductance, CO_2 exchange by the leaves and the flow of water through the soil and plants to the atmosphere. All simulations were for a crop with a leaf area index of 3 and a height of 0.8 m. Reference simulations used a uniform root length density of 4 km m^{-3}, a root depth of 1 m, root radius of 0.1 mm, a sandy loam soil and a constant plant hydraulic resistance of 1×10^7 MPa s m^{-1} (Sperry 2000). All model parameters are presented in Table 2.

Figure 2 shows the 24 h cycle of climatic data of air temperature (T_a), dew point temperature (T_r), wind speed (U), global and atmospheric long wave radiation (R_g, R_a) which were used in the simulations. This is an idealized day representative of typical clear summer conditions in temperate agricultural regions. During the day, R_g advances and declines symmetrically around noon; R_a remains essentially constant throughout the day and night period; T_a and T_r follow the course of the sun with a time lag of about 2 h

Table 2. Parameter values used to describe the vegetation and stomatal conductance in standard model runs

Parameter	Symbol	Value	Units
Vegetation			
Leaf area index	L_{AI}	3	m m^{-1}
Canopy height	h_c	0.8	m
Root depth	z_{root}	1	m
Root radius	r_{root}	0.1×10^{-3}	m
Plant hydraulic resistance	χ_v	1.10^7	MPa s m^{-1}
Average leaf width	d_l	0.01	m
Canopy mixing length	l_c	0.2	m
Stomatal conductance			
Residual conductance for CO_2	g_0	0.3×10^{-3}	mol m^{-2} s^{-1}
Parameter in g_{CO2} Eqn 1	a	2	

and U, which increases after sunrise, remains nearly constant throughout the day and decreases at sunset. All these climatic data refer to conditions 3 m above the ground.

Simulation results are presented for a 30 d drying cycle with an initial root zone uniformly wet ($\Psi_s = -0.05$ MPa). The meteorological forcing was repeated each day to simplify interpretation of predicted diurnal variations in stomatal conductance, assimilation, transpiration and leaf, root and soil water potentials.

RESULTS OF SIMULATIONS AND DISCUSSION

Time-course of the potentials ψ_s, ψ_r and ψ_v

The simulated diurnal variations in the water potentials of soil ψ_s, root ψ_r and leaf ψ_v, during a 30 d drying cycle are presented in Fig. 3. Initially, only the leaf water potential shows a marked variation during the day, accompanied by

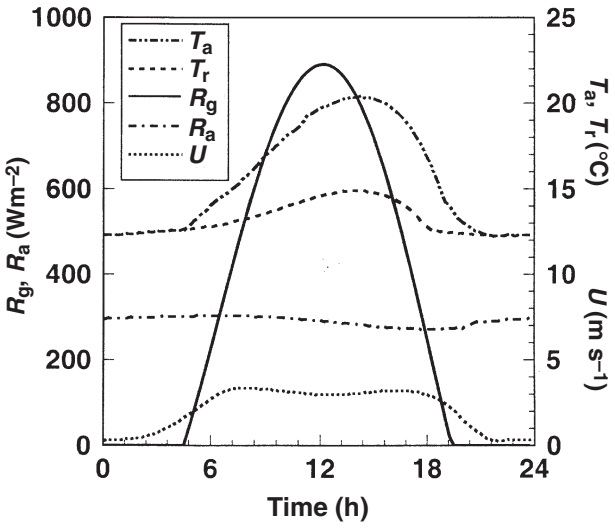

Figure 2. The 24 h cycle of climatic data of air temperature (T_a), dew point temperature (T_r), wind speed (U), global and atmospheric long wave radiation (R_g, R_a) used in the simulations.

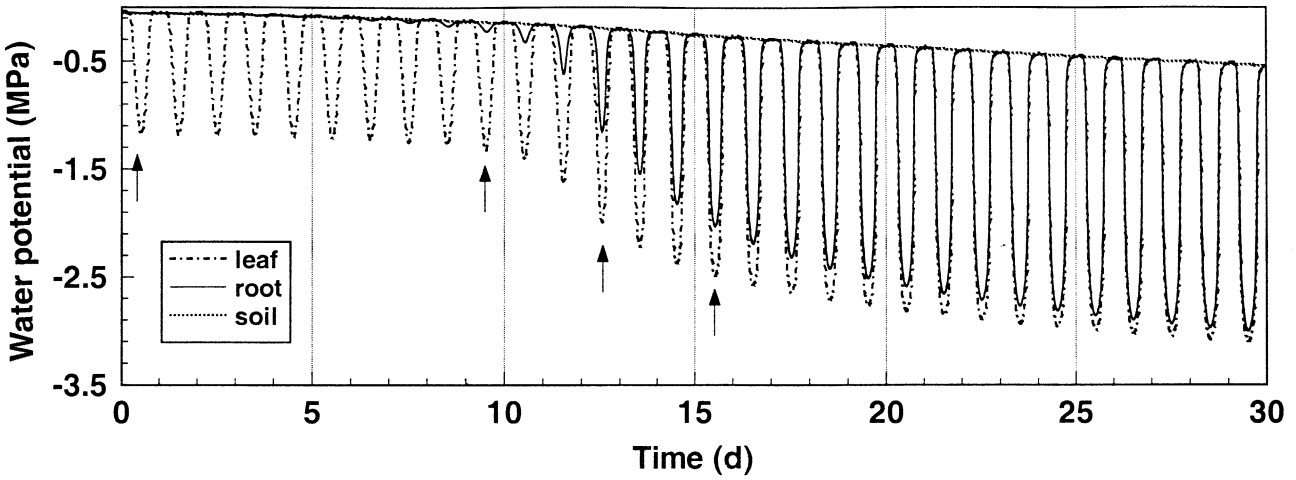

Figure 3. Time-course of leaf, root and soil water potentials during a 30 d drying cycle. The arrows indicate days of the drying cycle selected subsequently to show in more detail the diurnal changes of different variables.

a steady decline in root and soil water potentials. Soil water supply starts to limit transpiration after approximately 10 d of drying and values of ψ_r start to decrease rapidly due to a decrease of soil water content and soil hydraulic conductivity close to the roots. There is a lesser rate of decline in the minimum ψ_v, so the difference between ψ_v and ψ_r values gradually decrease throughout the drying cycle, leading to a reduction in water flow through the plants. The system equilibrates at night so that soil, root and leaf water potentials are equal. This value of ψ_s at night, which corresponds to the predawn water potential, decreases progressively throughout the drying cycle from the initial value of –0.05 MPa, to about –0.54 MPa after 30 d.

Predicted variations in soil water potential, ψ_s, as a function of distance from the roots, r, are shown in Fig. 4a at 3 h intervals for day 10 of the drying cycle. There is little variation in ψ_s with r around dawn (0600 h), but the potential near the roots progressively decreases during the day, reaching a minimum between 1200 and 1500 h. Matric potentials near the roots start to increase in the afternoon

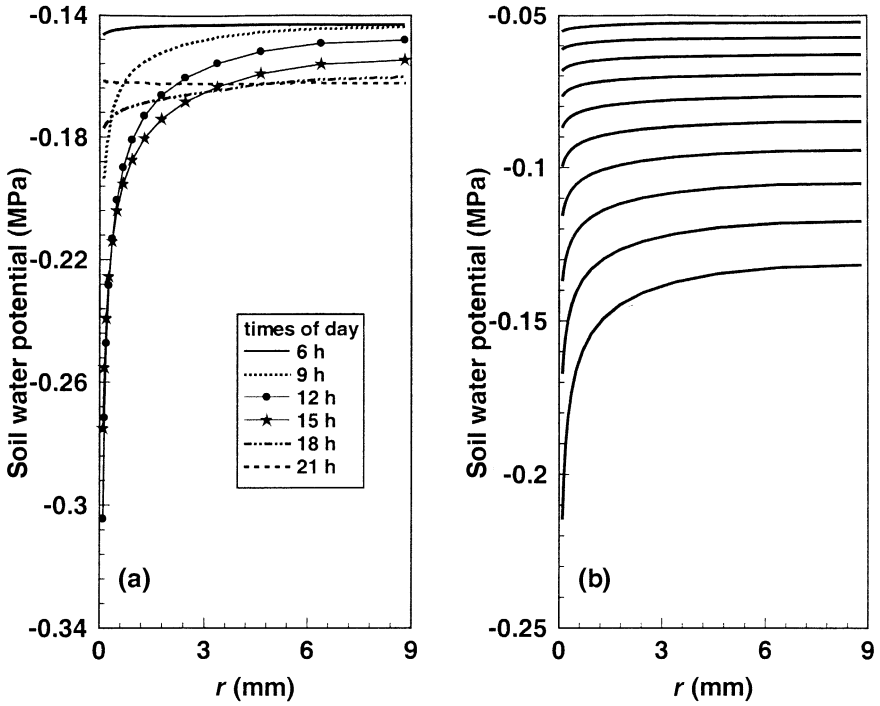

Figure 4. (a) The distribution of soil water potential, ψ_s, as a function of radial distance from the root, r, surface at 3 h intervals on day 10 of the drying cycle. (b) The distribution of ψ_s at noon as a function of r over a 10 d drying cycle (top to bottom)

as evaporative demand diminishes in late afternoon, and the ψ_s curves cross those of the morning as water in the root zone redistributes from the wetter regions in the bulk soil to the zone close to the roots. By late evening the potential is approximately uniform with distance but is at a lower value than the previous morning, commensurate with the extraction of soil water during the day. It is clear that the greatest changes in matric potential (and θ) occur close to the root surfaces. Hydraulic conductivity and resistance to water flow varies strongly with moisture content (Eqn 4b). Hence use of mean soil matric potentials will lead to incorrect values of resistance to water flow and will not capture the dynamics of the water transport as the soil dries.

Matric potentials decrease progressively as the soil dries, as shown in Fig. 4b for the predicted ψ_s profiles at noon during the first 10 d of the dry-down cycle. Initially there is little variation in ψ_s with distance, but as the soil dries ψ_s in the bulk soil decrease progressively whereas the potential near the roots decreases more strongly. These profiles are similar to those presented by Cowan (1965).

Diurnal changes of g_{CO2}, LE, A and c_i/c_s

Predicted diurnal variations in g_{CO2}, LE, A and the ratio c_i/c_s are shown in Fig. 5 for days 1, 10, 13 and 16 of the drying cycle. On day 1 when soil water availability is non-limiting, all quantities show a smooth and symmetrical variation around noon, with little or no asymmetry in these quantities caused by the peak in temperature and humidity deficit in mid-afternoon (Fig. 2) As soil moisture declines there is an increasingly asymmetrical pattern in g_{CO2}, A and LE, with values always higher in the morning than in the afternoon. This asymmetry is due to the lower leaf water potentials in the afternoon than in the morning, resulting from a higher atmospheric demand and a reduced ability of the soil to supply water to the roots because of lower matric potentials and hydraulic conductivity (Fig. 4). There is a close correlation in the patterns for g_{CO2} and A, which both showing a midday depression that becomes more pronounced as soil drying continues. The model shows that the proportional variation in A is less than in g_{CO2}. This is because the CO_2 concentration difference $(c_s - c_i)$ increases as the soil dries out, hence damping the variation in $A = g_{CO2}(c_s - c_i)$. The predicted midday depression is even less evident for LE than for A because the humidity deficit increases steadily with rising temperature from morning to mid-afternoon, counteracting the decrease in midday stomatal conductance. These predictions conform with the analysis of McNaughton & Jarvis (1983) which showed that LE is insensitive to canopy conductance for dense canopies. The general patterns in g_{CO2}, A and LE in response to soil drying shown in Fig. 5 are similar to reports in the literature as summarized by Schulze & Hall (1982) and Maier-Maercker (1998).

Soil drying also affects c_i/c_s. There is a small amplitude in c_i/c_s when soil water is adequate but a particularly strong

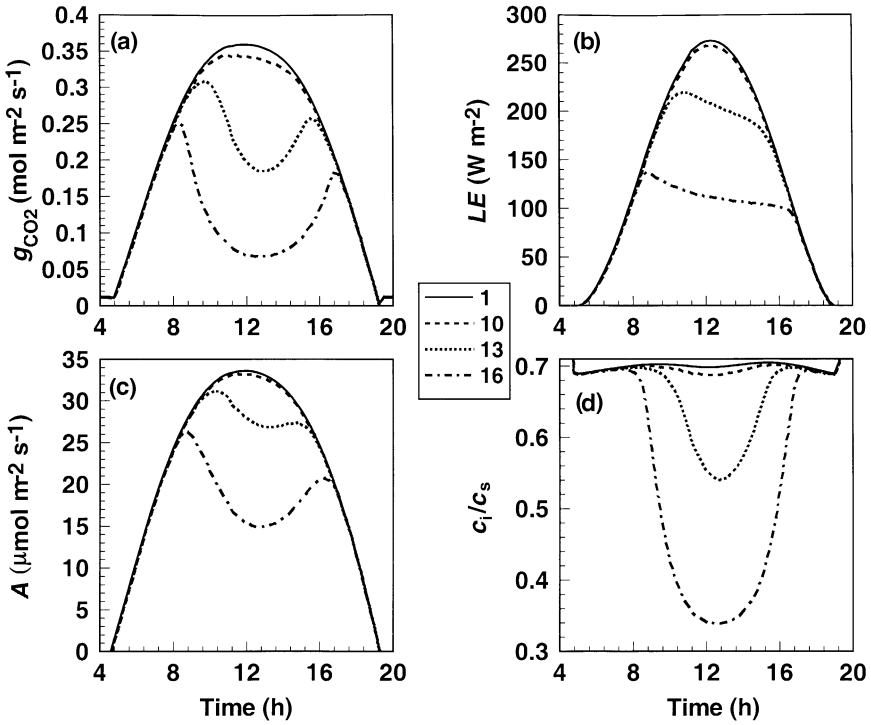

Figure 5. Diurnal variations of: (a) CO_2 stomatal conductance, (b) latent heat flux, (c) assimilation rate, and (d) the ratio of the CO_2 concentration in the intercellular spaces and the leaf surface for days 1, 10, 13 and 16 of the drying cycle. The asymmetry in the each quantity increases with the progression of the drying cycle and there is a marked midday depression predicted for g_{CO2} and A.

draw-down occurs later in the drying cycle (Fig. 5d). Such variation of c_i/c_s with increasing drought has been observed in the field for some species (Henson *et al*. 1989; Brodribb 1996; Eamus *et al*. 1999; Giorio, Sorrentino & d'Andria 1999). Patchy stomatal conductance or variation in photosynthetic capacity in response to drought causes c_i/c_s to remain constant in some other species (Forseth & Ehleringer 1983; Brodribb 1996). Such responses are not considered in this paper.

Sensitivity analysis

Sensitivity of stomatal conductance to leaf water potential

Stomata of different species vary in their sensitivity to leaf water potential, and three typical response curves are given in Fig. 6a. Curve (i) is typical of plants which are highly sensitive to leaf water potential, whereas curves (ii) and (iii) represents plants progressively more tolerant to water stress (cf. lupins and wheat in Henson *et al*. 1989). Evidence for the general shape of the functions may be found in Schulze & Hall (1982) and in the review by Leuning *et al*. (2003) which supports the hypothesis of Tyree & Sperry (1988), Jones & Sutherland (1991), Sperry (2000) and others, that stomata regulate leaf water potential to avoid xylem cavitation. Figure 6b. shows that species sensitive to leaf water potential [curve (i)] will have a smaller diurnal variation in ψ_v as the soil dries than less sensitive plants [curve (ii) or (iii)]. This figure shows that minimum leaf potentials are almost constant for type (i) plants, whereas the minimum ψ_v continues to decrease throughout the drying cycle for type (iii) plants.

The effect of variations in $f_{\psi v}$ on the relationship between g_{CO2} and ψ_v is presented in Fig. 6c for days 6, 15 and 20 of the drying cycle. We see that conductance is not a monotonic function of leaf water potential as may be expected from Fig. 6a, but follows a hysteresis loop, with higher g_{CO2} in the morning than in the afternoon for a given ψ_v. Hysteresis arises because stomatal conductance responds to multiple environmental and physiological factors (light, temperature, humidity deficit, intercellular CO_2 concentration) and because of the lower values of water potential at the root surfaces in the afternoon than in the morning as discussed above. The model predicts a lower maximum stomatal conductance, and a tighter hysteresis loop between g_{CO2} and ψ_v on each day for plant type (i) than for (ii) and (iii). There is also a progressive decrease in the maximum stomatal conductance as soil drying proceeds, but differences in $g_{CO2,\,max}$ for the various $f_{\psi v}$ are small by day 20 (Fig. 6c).

Sensitivity of leaf water potential and stomatal conductance to plant hydraulic resistance

Figure 7 shows the sensitivity of ψ_v and g_{CO2} to three values of plant hydraulic resistance: $\chi_v = 0.25 \times 10^7$, 0.5×10^7 and

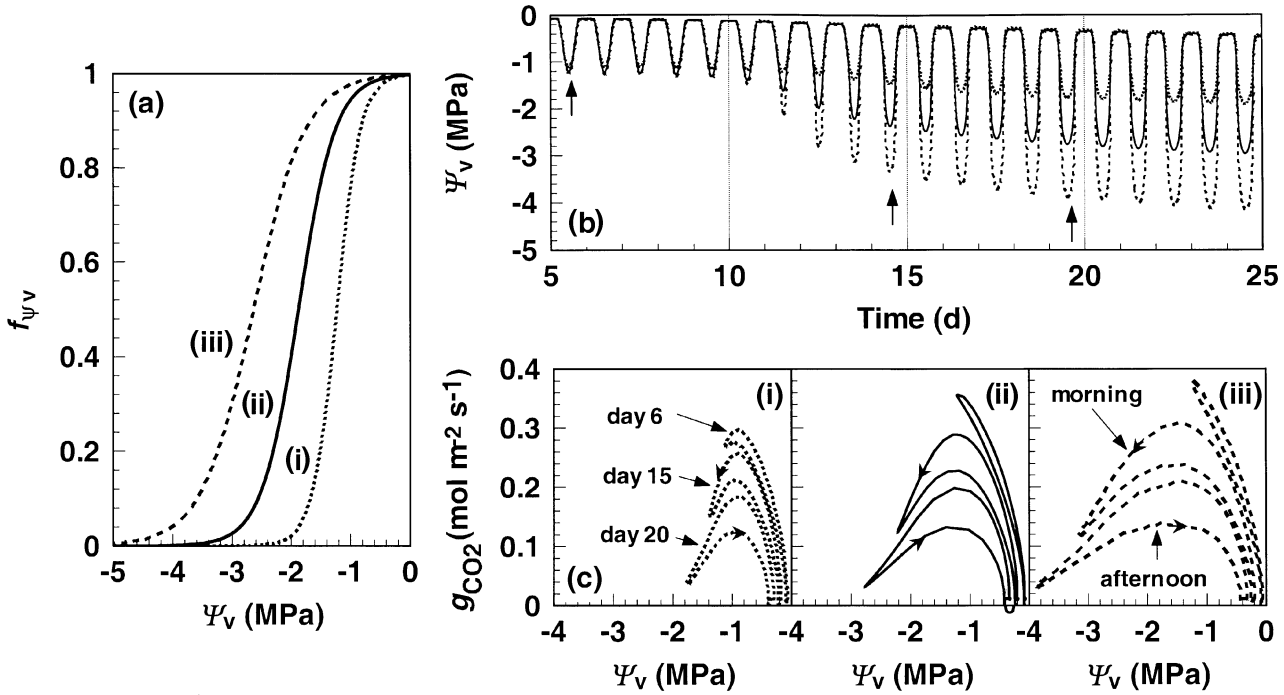

Figure 6. (a) Three different functions describing the sensitivity of stomatal conductance to ψ_v [(I) $s_f = 4.9$, $\psi_f = -1.2$; (ii) $s_f = 3.2$, $\psi_f = -1.9$; (iii) $s_f = 2.3$, $\psi_f = -2.6$]. (b) Predicted diurnal variations in leaf water potential ψ_v as the soil dries for the three stomatal functions. (c) The relationship between g_{CO2} and ψ_v for days 6, 15 and 20, for each of the $f_{\psi v}$ functions. The first 5 d of the simulation have been omitted in (b) because during that period the model predicts no differences between the different functions.

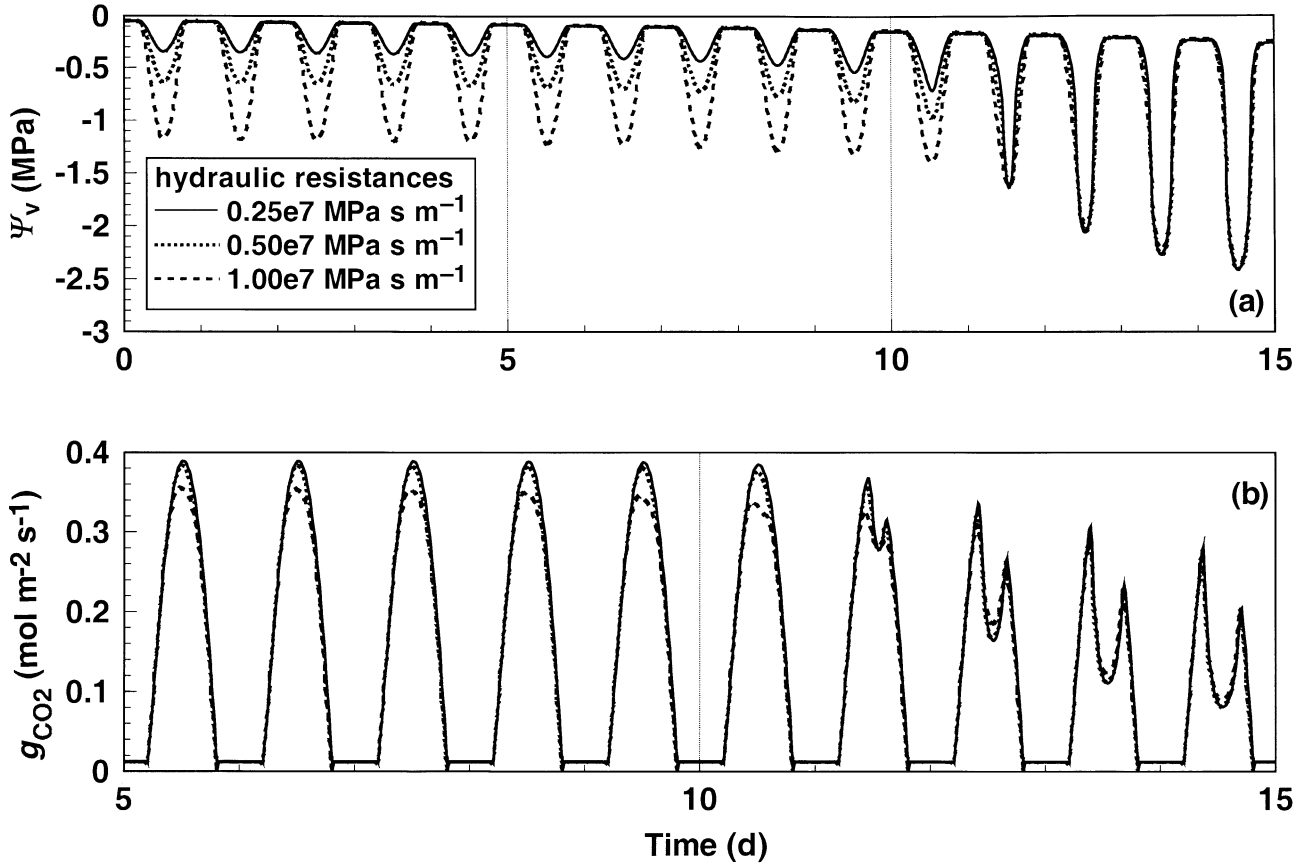

Figure 7. Sensitivity of (a) leaf water potential and (b) stomatal conductance for CO_2 to three values of plant hydraulic resistance. The first 5 d of the simulation have been omitted in (b) because the model predicts no differences between plant hydraulic resistances during that period.

1.0×10^7 MPa s m^{-1}. Early in the drying cycle when soil moisture is not limiting, the simulations indicate that the minimum daytime value ψ_v depends strongly on χ_v. For a given transpiration rate, lower hydraulic resistance results in less negative leaf water potentials and higher stomatal conductances. The relatively small response of g_{CO2} to variation in ψ_v at high soil moisture contents is because of the 'shoulder' in the function $f_{\psi v}$ at potentials near zero (Fig. 6a). The rate of soil water supply to the roots starts to limit transpiration around day 11 and there is a progressive decrease of both ψ_v and g_{CO2}, with midday depressions in the latter becoming increasingly evident (Fig. 7). At this stage of the drying cycle, there is little effect of hydraulic resistance on leaf water potential and stomatal conductance, because soil moisture limits supply. Leaf and root potentials also become very similar at this time (Fig. 3).

These simulations are examples of 'anisohydric' plants as defined by Tardieu & Simonneau (1998). In these plants, minimum daytime leaf water potential continues to decrease when the soil dries out. In contrast, 'isohydric' plants appear to maintain an approximately constant minimum daytime leaf water potential throughout the drying cycle. Anisohydric plants are expected to have low hydraulic resistance, χ_v, and/or low-to-moderate stomatal sensitivity to leaf water potential, s_f (Fig. 6) whereas isohydric plants are expected to have high χ_v, and/or higher s_f. Tardieu & Davies (1993) and Dewar (2002) explained these results through the combined roles of the hormone abscisic acid (ABA) and the supply and loss of water to/from the leaves on stomatal conductance. While not denying a role of ABA in regulating stomatal aperture at the cellular level, the present model is able to explain the contrasting behaviour of anisohydric and isohydric plants in terms of differing plant hydraulic resistances and stomatal sensitivities of stomata to leaf water potential, without explicitly invoking hormonal control.

Sensitivity of stomatal conductance and cumulative transpiration to soil characteristics

Predictions for g_{CO2} and cumulative soil water consumption during a 30 d drying cycle are shown in Fig. 8 for three soil types: loam, silt loam and sandy loam (see Table 1 for soil parameter values). Stomatal conductance is insensitive to soil type during the first 10 d of drying (results not shown). Conductances for plants in sandy loam then begin to respond to soil drying, showing a rapid decrease each day and marked midday depressions. However, reduction in

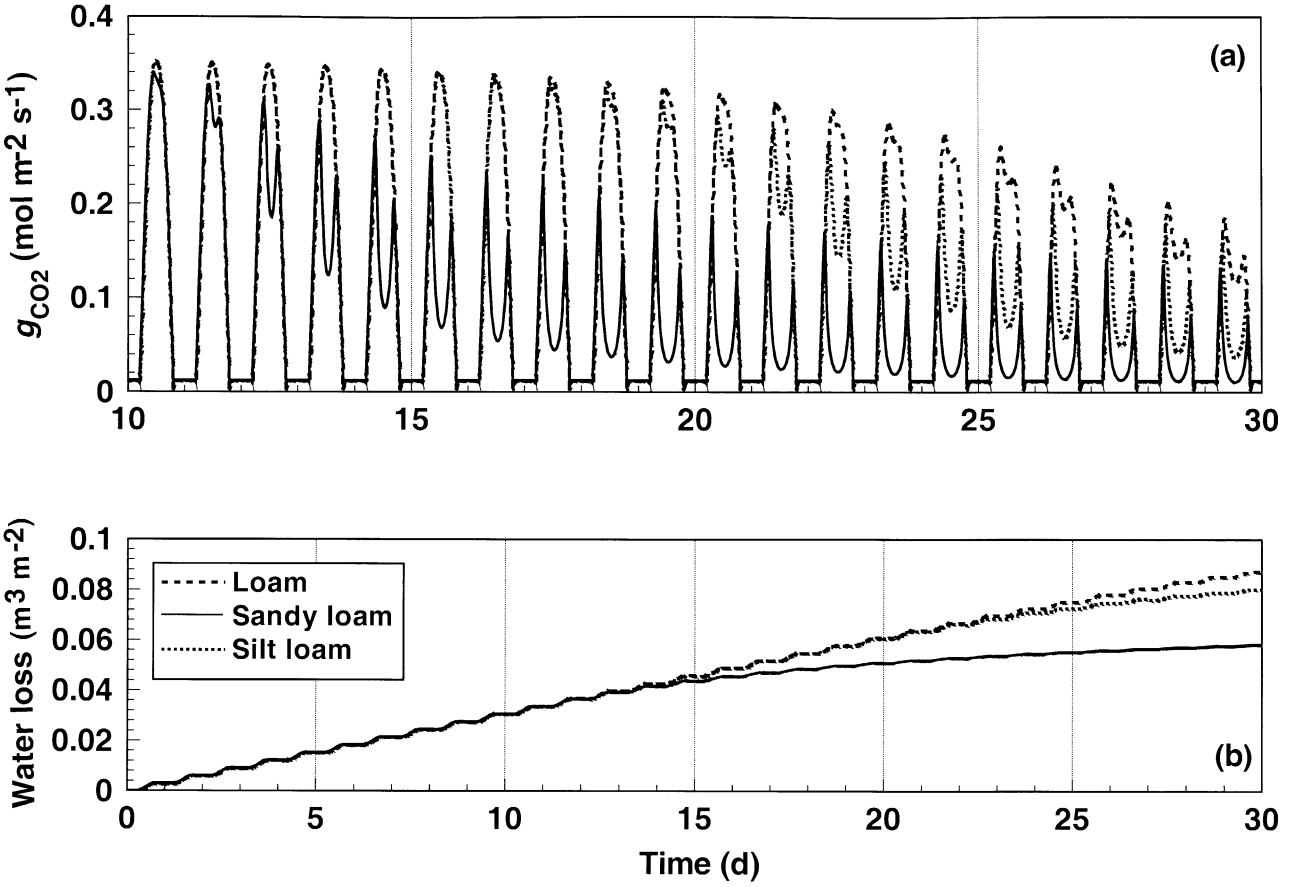

Figure 8. Sensitivity of (a) stomatal conductance, and (b) cumulative transpiration to soil type with hydraulic characteristics given in Table 1. The first 10 d of the simulation have been omitted in (a) because the model predicts no differences between soil types during that period.

cumulative transpiration rates are observed only 4 d later. A similar picture is seen for the silt loam and loam soils, except that the onset of soil limitation to conductance and transpiration occurs progressively later. Differences in the responses of stomatal conductance to soil type are a function of their moisture retention characteristics, with matric potential dropping more rapidly at low moisture contents in the order sandy loam, loam and then silt loam. This causes leaf water potential and stomatal conductance to decrease in the same order.

Sensitivity of stomatal conductance and cumulative transpiration to root densities

The sensitivity of g_{CO2} and soil water consumption to root length density is presented in Fig. 9. These results correspond to three values of root length density: 2, 4 and 6 km m^{-3} in silty loam during a 30 d drying cycle. The first 5 d of the simulation have been omitted from the top panel because the model predicts no differences between root densities during that period. Small differences in conductance appear after day 7 of drying, but differences in transpiration are evident only after 11 d. Higher root length densities maintain higher stomatal conductances only from days 8–17, after which lack of soil water causes similar limitations to stomatal conductance, irrespective of root length density.

Transpiration rates as a function of soil moisture and atmospheric demand

So far we have focused on relationships between stomatal conductance, transpiration and water potential gradients between the soil, root and leaves, during a soil drying cycle. However, it is also possible to consider the role of soil water content in controlling transpiration, since soil water potential and water content are related through the moisture retention curve (Eqn 4). In a classic paper, Denmead & Shaw (1962) hypothesized that leaf wilting, and hence stomatal closure, will occur at higher soil moisture contents when atmospheric demand for water vapour increases. This is expected to occur because the moisture content immediately around the roots will be rapidly depleted at high atmospheric demand and the decrease of soil conductivity will mean that the soil will not be able to supply the water

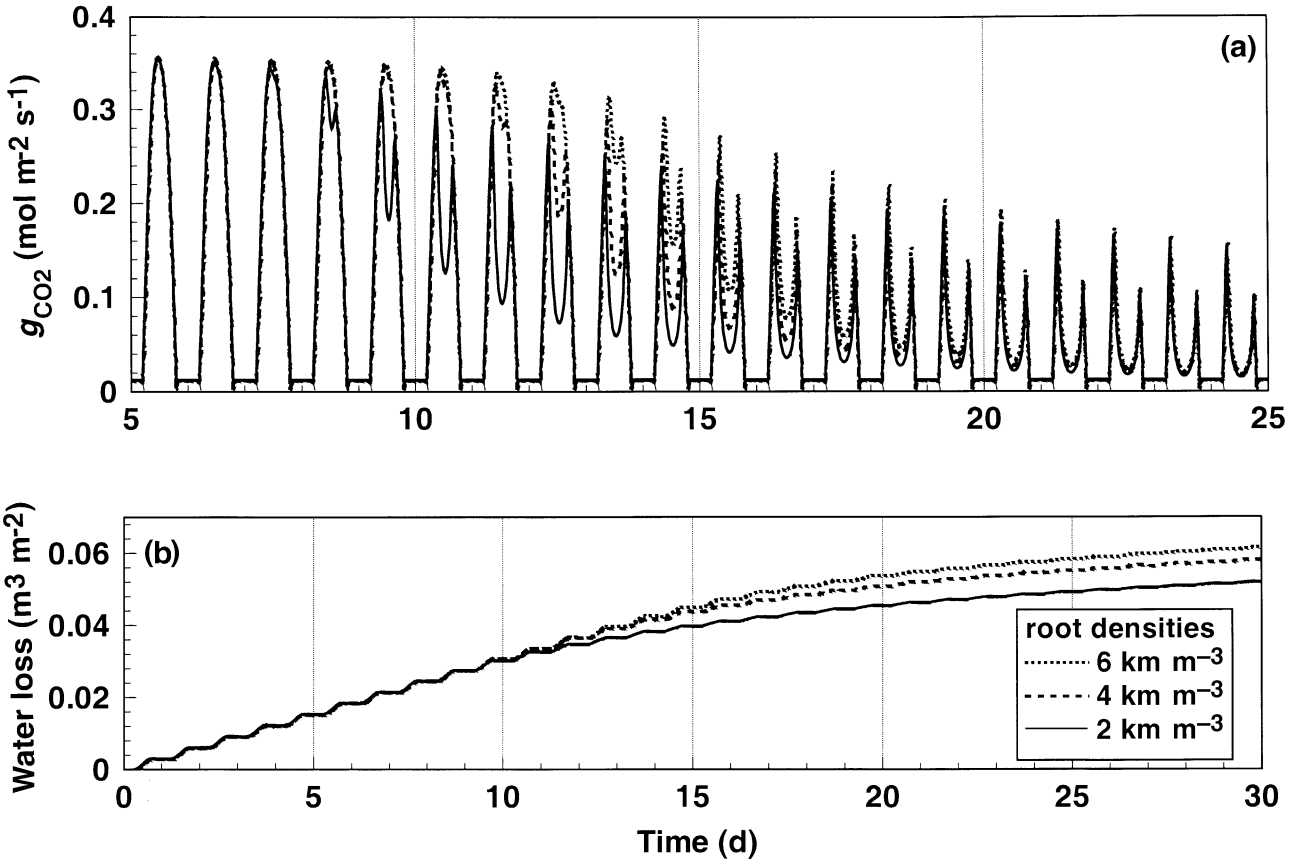

Figure 9. Sensitivity of (a) stomatal conductance, and (b) cumulative transpiration to root densities. The first 5 d of the simulation have been omitted in (a) because the model predicts no differences between root densities during that period.

sufficiently quickly (Fig. 4). Leaf water potential will also be lower at high transpiration rates. To support this hypothesis, Denmead & Shaw (1962) showed that transpiration rates declined at higher soil moisture contents when atmospheric demand was high, compared to when demand was low.

We attempted to simulate these results using the current model and the results are shown in Fig. 10a for transpiration rate as a function of soil moisture content and evaporative demand. Because the transpiration rate varies during the day, only the midday values are plotted, to emphasize the changes from day to day. Contrary to the findings of Denmead and Shaw, the model shows there is no cross-over of the curves, although there is a suggestion that *LE* does start to decline at a higher soil moisture content when demand is high compared to when it is low. However, the predicted transition from energy-limited transpiration (approximately horizontal part of curve) to limitation by soil water supply occurs over a rather narrow moisture content range. Cross-over of the curves is found when *LE* is plotted as a function of time (Fig. 10b). Longer times correspond drier soils, so it appears that the results of Denmead & Shaw (1962) can be explained if their graph is a composite derived from plants which started transpiration at different initial moisture contents.

Response of g_{CO2}, *LE*, *A* and c_i/c_s to humidity deficit at the leaf surface

It was seen in Fig. 6c that a plot of the diurnal variation g_{CO2} versus ψ_v shows hysteresis, even though the relationship between g_{CO2} and ψ_v used in the stomatal model is monotonic (Eqn 2, Fig. 6a). Hysteresis occurs because conductance depends simultaneously on multiple factors such as light, temperature, intercellular CO_2 concentration and water flow through the soil and plant. Similarly, no unique relationships are expected between g_{CO2}, *LE*, *A* and c_i/c_s and humidity deficit at the leaf surface, D_s (Fig. 11) when multiple factors vary concurrently. Each curve shows hysteresis, the degree of which depends on the above factors. During a daily cycle, the model predicts that g_{CO2} and D_s are positively correlated at low values of D_s when absorbed light largely controls conductance through photosynthesis, whereas there is a negative correlation between g_{CO2} and D_s later in the day (Fig. 11a). Conductances are higher in the morning than in the afternoon at the same value of D_s because soil matric potential around the roots differs from morning and afternoon (Fig. 4). Such hysteresis has been observed by Pereira, Tenhunen & Lange (1987), Takagi, Tsuboya & Takahashi (1998), Eamus *et al.* (1999) and by Meinzer *et al.* (1997) for a variety of plant species when

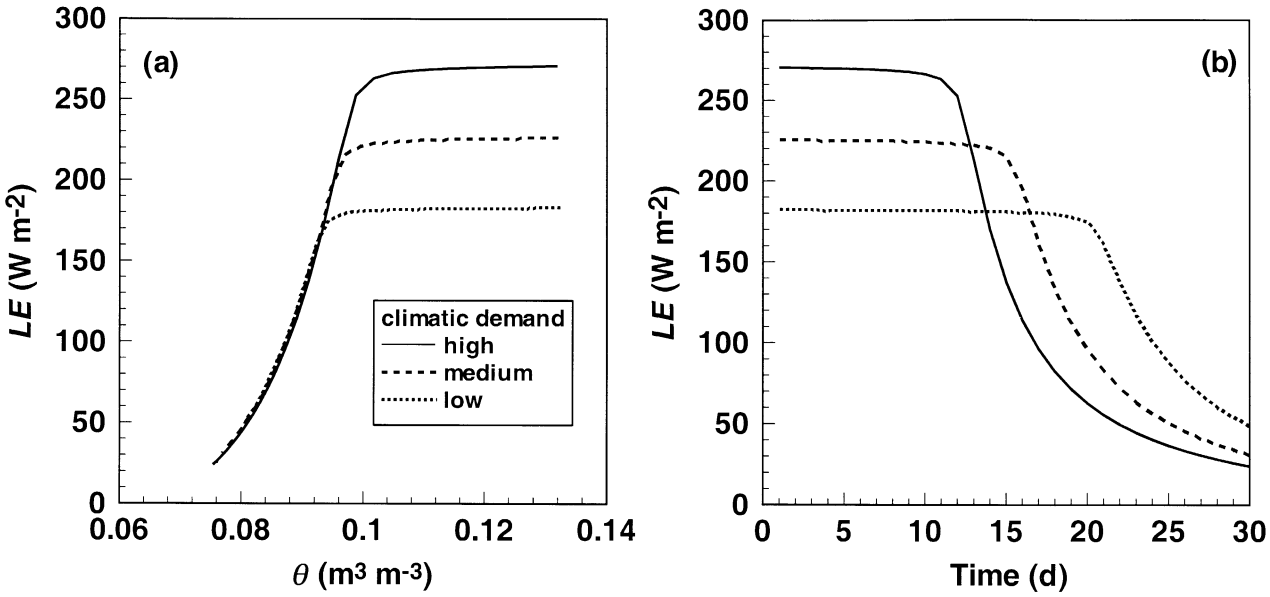

Figure 10. Maximum daily transpiration rates as a function of (a) soil moisture content, and (b) time, for three different levels of atmospheric evaporative demand. The diurnal variation of climatic demand used in these simulations have a mean daytime value equal to: 201, 237 and 274 W m^{-2}.

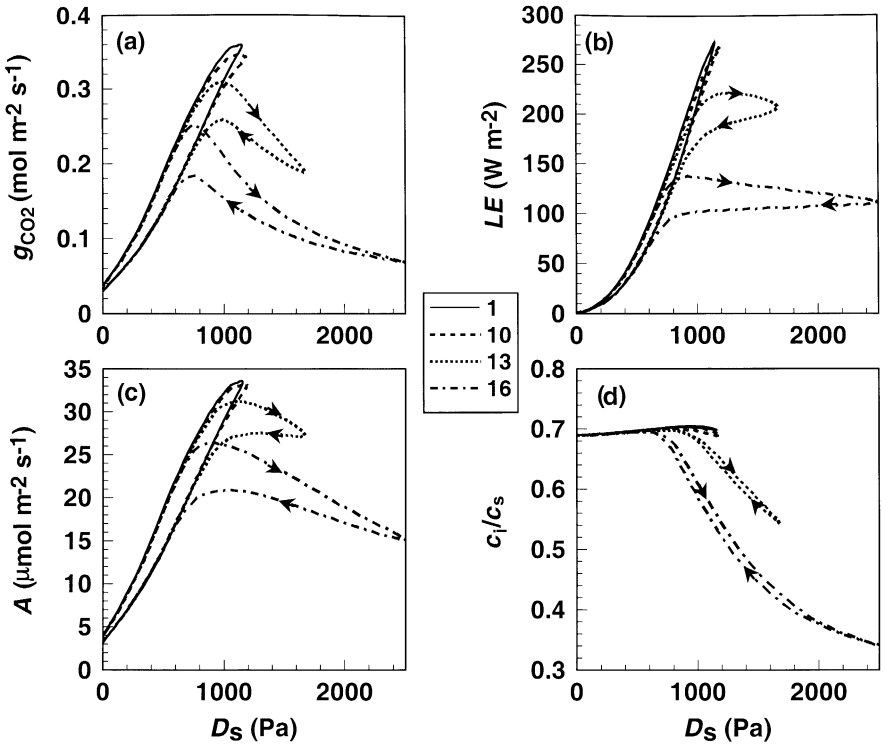

Figure 11. Predicted relationships between humidity deficit at the leaf surface and: (a) stomatal conductance; (b) transpiration rate; (c) assimilation rate; and (d) the ratio of the CO_2 concentration in the intercellular spaces and the leaf surface for days 1, 10, 13 and 16 of the drying cycle. The model predicts hysteresis in all the relationships shown as a result of multiple factors such as light, temperature, intercellular CO_2 concentration and water flow through the soil and plant.

measurements were made in the field. According to the model presented here, the hyperbolic relationship between g_{CO2} and D_s used by Lohammer *et al.* (1980) and by Leuning (1995) is apparent only at high values of D_s once soil moisture starts to limit water supply to the roots. Note that the maximum value of D_s increases from day 1 to day 16, despite the use of the same maximum atmospheric humidity deficit at the reference height. This occurs because D_s depends on interactions between stomatal conductance, transpiration rate and leaf temperature through the leaf energy balance.

Transpiration rates (LE) are positively correlated with D_s throughout the day early in the drying cycle, but once soil water supply becomes limiting (days 13 and 16 in Fig. 11b), LE is negatively correlated to D_s from mid-morning to mid-afternoon and then insensitive to D_s later in the day. Similar trends are observed in the relationship between A and D_s, except that the negative correlation is more apparent at low water contents than it is for LE (Fig. 11c). Intercellular CO_2 concentrations are relatively independent of D_s at high soil moisture contents, but are predicted to decrease markedly later in the drying cycle (Fig. 11d). Evidence of diurnal hysteresis in some or all of g_{CO2}, LE, A and c_i/c_s under field conditions when plotted against, time of day, humidity deficit and leaf water potential may be found in Schulze & Hall (1982), Beadle *et al.* (1985), Henson *et al.* (1989), Brodribb (1996) and Meinzer *et al.* (1997).

Dependence of *A* and *LE* on g_{CO2}

The predicted dependence of A and LE on g_{CO2} is shown in Fig. 12 for several days during a drying cycle when all factors controlling stomatal conductance co-vary. The relationship between A and g_{CO2} is approximately linear when soil water is non-limiting (Fig. 12a), implying an approximately constant value of c_i (Fig. 11d). Hysteresis appears in the relationship by day 13 and the spread in the hysteresis curve increases as the soil dries out, yielding results similar to those presented by Schulze & Hall (1982) and Pereira *et al.* (1987) for observations made under field conditions.

There is also hysteresis in the predicted relationship between LE and g_{CO2} (Fig. 12b), very similar to results presented by Meinzer *et al.* (1997). Transpiration and g_{CO2} are positively correlated throughout the day when soil moisture is adequate, but for moderately dry soils LE remains approximately constant whereas g_{CO2} declines between mid-morning and mid-afternoon. There is some recovery of stomatal conductance after the midday depression in these simulations, but LE continues to decline with reduced atmospheric demand late in the afternoon (cf. Figs 5 & 12b). Farquhar (1978) argued that simple feedback between g_{CO2} and D_s was unable to account for a decrease in LE with decreasing g_{CO2} and postulated that stomata must sense water stress by mechanism(s) that involve more than transpiration (so-called 'feed-forward' response). Our model shows that it is unnecessary to invoke a feed-forward response of stomata to D_s, when stomatal conductance is a function of leaf water potential and the dynamics of the resistance to water transport from soil to roots is included in the model. Hydraulic resistance can vary due to changes in soil hydraulic conductivity with soil moisture content around the roots and with water potential-dependent cavitation in the xylem (Sperry 2000; Buckley & Mott 2002).

CONCLUSIONS

A fully coupled soil-plant-atmosphere continuum model has been developed in which stomatal conductance is a function of photosynthesis, intercellular CO_2 concentration and leaf water potential. The latter in turn depends on soil water potential, the flux of water through the soil and plant, xylem hydraulic resistance and hence stomatal conductance. Diurnal patterns of leaf water potential, absorption of water by roots, canopy transpiration and photosynthesis are predicted by the model using specified meteorological variables, soil water content and canopy and soil characteristics.

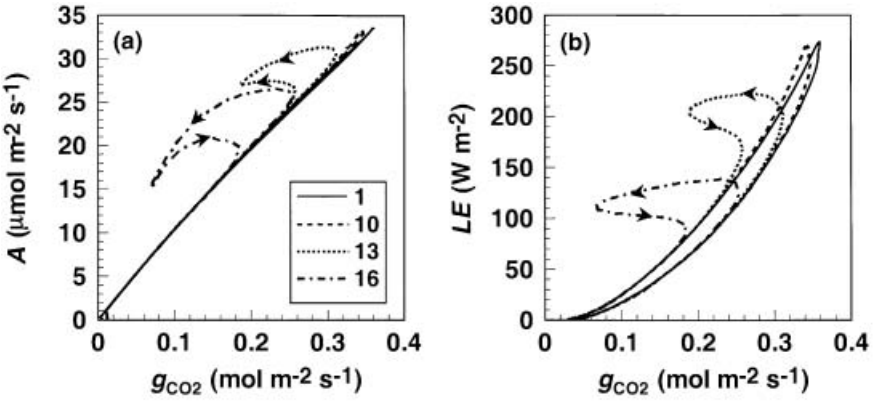

Figure 12. Predicted relationships between stomatal conductance for CO_2 and: (a) assimilation rate and (b) transpiration rate for days 1, 10, 13 and 16 of the drying cycle. Hysteresis occurs in the relationships because of interactions of multiple factors.

The model reproduces the observed diurnal variation in stomatal conductance, assimilation rate and transpiration for a typical crop. It successfully captures the daytime asymmetry in conductance, assimilation and transpiration under water stress conditions and it describes successfully the observed hysteresis in stomatal conductances versus leaf water potential. Hysteresis occurs because leaf water potential is a function of the dynamics in the distribution of soil matric potential around the roots. Once soils start to dry, matric potentials close to the roots are less negative in the morning than in the afternoon and thus, for a given level of atmospheric demand for water from the leaves, stomatal conductances are higher earlier in the day.

The model shows that 'isohydric' plants, which maintain constant minimum leaf water potentials, are expected have high xylem hydraulic resistance and/or high stomatal sensitivity to leaf water potential. 'Anisohydric' plants, which have variable minimum leaf water potentials, are expected to have lower hydraulic resistances and/or lower stomatal sensitivity to leaf water potential.

Model sensitivity analysis for a soil dry-down cycle of 30 d shows that stomatal conductance depends on soil and plant hydraulic properties and root length density. Variation in these model parameters cause differences in stomatal conductance and leaf water potential to appear only after approximately 10 d of drying, when supply of water by the soil to the roots becomes limiting. High atmospheric demand causes transpiration rate, LE, to decline at a slightly higher soil water content, θ_s, than at low atmospheric demand, but all curves of LE versus θ_s fall on the same line when soil water supply limits transpiration. The model emphasizes that stomatal conductance cannot be modelled in isolation, but must be fully coupled with photosynthesis/respiration and the transport of water from soil, through roots, stems and leaves to the atmosphere.

The above results may be criticised because the model is too simple or that no direct experimental evidence has been presented in support of the model. The model has deliberately been kept simple to emphasize the key processes involved in stomatal control of the coupled exchanges of $CO_{2\ and}$ water vapour between plants and the atmosphere. For example, the model does not separate the canopy into sunlit and shaded leaves (cf. DePury & Farquhar 1997; Wang & Leuning 1998), and uses a single, homogeneous soil layer with a uniform root distribution. Phenomena such as patchy stomatal conductance or reductions in photosynthetic capacity with drought have also not been considered. Despite these limitations, the model successfully predicts patterns in the diurnal variation of g_{CO2}, LE, A and c_i/c_s widely observed under field conditions for plants in well-watered and drying soils. However, it is not possible to verify the model with a single experiment. The details of the response for a given experiment will vary considerably, depending on a combination of meteorology, plant physiology (e.g. photosynthetic capacity, hydraulic resistance), canopy density, soil moisture content and soil hydraulic properties. The key conclusion of the paper is that stomatal conductance cannot be modelled using leaf-level processes alone, but must be incorporated into a comprehensive model of CO_2 exchange by leaves and water flow from soil through the plants to the atmosphere.

REFERENCES

Amthor J.S. (1994) Scaling CO_2-photosynthesis relationships from the leaf to the canopy. *Photosynthesis Research* **39,** 321–350.

Anderson M.C., Norman J.M., Meyers T.P. & Diak G.R. (2000) An analytical model for estimating canopy transpiration and carbon assimilation fluxes based on canopy light-use efficiency. *Agricultural and Forest Meteorology* **101,** 265–289.

Assmann S.M. (1999) The cellular basis of guard cell sensing to rising CO_2. *Plant, Cell and Environment* **22,** 629–637.

Baldocchi D. & Meyers T. (1998) On using eco-physiological, micrometeorological and biogeochemical theory to evaluate carbon dioxide, water vapor and trace gas fluxes over vegetation: a perspective. *Agricultural and Forest Meteorology* **90,** 1–25.

Ball J.T., Woodrow I.E. & Berry J.A. (1987) A model predicting stomatal conductance and its contribution to the control of photosynthesis under different environmental conditions. In *Progress in Photosynthesis Research* (ed. I. Biggens), pp. 221–224. Martinus-Nijhoff Publishers, Dordrecht, The Netherlands.

Beadle C.L., Talbot H., Neilson R.E. & Jarvis P.R. (1985) Stomatal conductance and photosynthesis in a mature Scots pine forest. III. Variation in canopy conductance and canopy photosynthesis. *Journal of Applied Ecology* **22,** 587–595.

Blatt M.R. (2000) Cellular signaling and Volume control in stomatal movements in plants. *Annual Review of Cell Development Biology* **16,** 221–241.

Bond B. & Kavanagh K.L. (1999) Stomatal behavior of four woody species in relation to leaf-specific hydraulic conductance and threshold water potential. *Tree Physiology* **19,** 503–510.

Brodribb T. (1996) Dynamics of changing intercellular CO_2 concentration (c_i) during drought and determination of minimum functional c_i. *Plant Physiology* **111,** 179–185.

Buckley T.N. & Mott K.A. (2002) Stomatal water relations and the control of hydraulic supply and demand. *Progress in Botany* **63,** 309–325.

Calvet J.-C., Noilhan J., Roujean J.-L., Bessemoulin P., Cabelguenne M., Olioso A. & Wigneron J.-P. (1998) An interactive SVAT model tested against data from six contrasting sites. *Agricultural and Forest Meteorology* **92,** 73–95.

Campbell G.S. (1985) *Soil Physics with Basic: Transport Models for Soil-Plant Systems*. Elsevier. Science Publishers, Amsterdam, The Netherlands.

Choudhury B.J. & Monteith J.L. (1988) A four-layer model for the heat budget of homogeneous land surfaces. *Quarterly Journal of the Royal Meteorological Society* **114,** 373–398.

Collatz G.J., Ball J.T., Grivet C. & Berry J.A. (1991) Physiological and environmental regulation of stomatal conductance, photosynthesis and transpiration: a model that includes a laminar boundary layer. *Agricultural and Forest Meteorology* **54,** 107–136.

Comstock J. & Mencuccini M. (1998) Control of stomatal conductance by leaf water potential in *Hymenoclea salsola* (T. & G.), a desert shrub. *Plant, Cell and Environment* **21,** 1029–1038.

Cowan I.R. (1965) Transport of water in the soil-plant-atmosphere continuum. *Journal of Applied Ecology* **2,** 221–239.

Cowan I.R. (1977) Stomatal behaviour and environment. *Advances in Botanical Research* **4,** 117–228.

Denmead O.T. & Shaw R.H. (1962) Availability of soil water to plants as affected by soil moisture content and meteorological conditions. *Agronomy Journal* **54,** 385–390.

DePury D.G.G. & Farquhar G.D. (1997) Simple scaling of

photsynthesis from leaves to canopies without the errors of big-leaf models. *Plant, Cell and Environment* **20,** 537–557.

Dewar R.C. (2002) The Ball-Berry-Leuning and Tardieu-Davies models: synthesis and extension at guard cell level. *Plant, Cell and Environment* **19,** 1383–1398.

Eamus D., Myers B., Duff G. & Williams D. (1999) Seasonal changes in photsynthesis of eight savanna tree species. *Tree Physiology* **19,** 665–671.

Eamus D., Hutley L.B. & O'Grady A.P. (2001) Daily and seasonal patterns of carbon and water fluxes above a north Australian savanna. *Tree Physiology* **21,** 977–988.

Farquhar G.D. (1978) Feedforward responses of stomata to humidity. *Australian Journal of Plant Physiology* **5,** 787–800.

Farquhar G.D. & Wong S.C. (1984) An empirical model of stomatal conductance. *Australian Journal of Plant Physiology* **11,** 191–210.

Farquhar G.D., Caemmerer von S. & Berry J.A. (1980) A biochemical model of photosynthetic CO_2 assimilation in leaves of C3 species. *Planta* **149,** 78–90.

Forseth I.N. & Ehleringer J.R. (1983) Ecopyhsiology of two solar tracking desert winter annuals III. Gas exchange responses to light, CO_2 and VPD in relation to long-term drought. *Oecologia* **57,** 344–351.

Franks P.J., Buckley T.N., Shope J.C. & Mott K.A. (2001) Guard cell Volume and pressure measured concurrently by confocal microscopy and the cell pressure probe. *Plant Physiology* **125,** 1577–1584.

Gardner W.R. (1960) Dynamic aspects of water availability to plants. *Soil Science* **89,** 63–73.

Giorio P., Sorrentino G. & d'Andria R. (1999) Stomatal behaviour, leaf water status and photsynthetic response of field-grown olive trees under water deficit. *Environmental and Experimental Botany* **42,** 95–104.

Grant R.F., Wall G.W., Kimball B.A., Frumau K.F.A., Pinter P.J. Jr, Hunsaker D.J. & Lamorte R.L. (1999) Crop water relations under different CO_2 and irrigation: testing of *ecosys* with the free air CO_2 enrichment (FACE) experiment. *Agricultural and Forest Meteorology* **95,** 27–51.

Harley P.C., Thomas R.B., Reynolds J.F. & Strain B.R. (1992) Modelling photosynthesis of cotton grown in elevated CO_2. *Plant, Cell and Environment* **15,** 271–282.

Henson I.E., Jensen C.R. & Turner N.C. (1989) Leaf gas exchange and water relations of lupins and wheat. I. Shoot response to soil water deficits. *Australian Journal of Plant Physiology* **16,** 401–413.

Inoue E. (1963) On the turbulent structure of airflow within crop canopies. *Journal of the Meteorological Society of Japan* **41,** 317–326.

Jarvis P.G. (1976) The interpretation of the variations in leaf water potential and stomatal conductance found in canopies in the field. *Philosophical Transactions of the Royal Society of London Series B-Biology Sciences* **273,** 593–610.

Jensen C.R., Svendsen H., Andersen M.N. & Lösch R. (1993) Use of the root contact concept, an empirical leaf conductance model and pressure-volume curves in simulating crop water relations. *Plant and Soil* **149,** 1–26.

Jones H.G. & Sutherland R.A. (1991) Stomatal control of xylem embolism. *Plant, Cell and Environment* **14,** 607–612.

Leuning R. (1990) Modelling stomatal behavior and photosynthesis of *Eucalyptus grandis*. *Australian Journal of Plant Physiology* **17,** 159–175.

Leuning R. (1995) A critical appraisal of a combined stomatal-photosynthesis model for C_3 plants. *Plant, Cell and Environment* **18,** 339–355.

Leuning R. (1997) Scaling to a common temperature improves the correlation between photosynthesis parameters J_{max} and V_{cmax}. *Journal of Experimental Botany* **307,** 345–347.

Leuning R., Dunin F.X. & Wang Y.-P. (1998) A two-leaf model for canopy conductance, photosynthesis and partitioning of available energy. II. Comparison with measurements. *Agricultural and Forest Meteorology* **91,** 113–125.

Leuning R., Kelliher F.M., DePury D.G.G. & Schulze E.-D. (1995) Leaf nitrogen, photosynthesis, conductance and transpiration: scaling from leaves to canopies. *Plant, Cell and Environment* **18,** 1183–1200.

Leuning R., Tuzet A. & Perrier A. (2003) Stomata as part of the soil-plant-atmosphere continuum. In *Forests at the Land–Atmosphere Interface* (eds M. Mencuccini, J. Grace, J. Moncrieff, K. McNaughton). CAB International, Edinburgh, Scotland.

Lohammer T., Larsson S., Linder S. & Falk S.O. (1980) FAST-Simulation models of gaseous exchange in scots pine. *Ecology Bulletin* **32,** 505–523.

Maier-Maercker U. (1998) Dynamics of change in stomatal response and water status of *Picea abies* during a persistent drought period: a contribution to the traditional view of plant water relations. *Tree Physiology* **18,** 211–222.

Maier-Maercker U. (1999) New light on the importance of peristomatal transpiration. *Australian Journal of Plant Physiology* **26,** 9–16.

McMurtrie R.E., Leuning R., Thompson W.A. & Wheeler A.M. (1992) A model of canopy photosynthesis and water use incorporating a mechanistic formulation of leaf CO_2 exchange. *Forest Ecology and Management* **52,** 261–278.

McNaughton K.G. & Jarvis P.G. (1983) Predicting effects of vegetation changes on transpiration and evaporation. In *Water Deficits and Plant Growth Vol. 7* (ed. T.T. Kozlowski), pp. 1–47. Academic Press New York, USA.

Meinzer F.C., Andrade J.L., Goldsteein G., Holbrook N.M., Cavelier J. & Jackson P. (1997) Control of transpiration from the upper canopy of a tropical forest: the role of stomatal, boundary layer and hydraulic architecture components. *Plant, Cell and Environment* **20,** 1242–1252.

Mencuccini M., Mambelli S. & Comstock J. (2000) Stomatal responsiveness to leaf water status in common bean (*Phaseolus vulgaris* L.) is a function of time of day. *Plant, Cell and Environment* **23,** 1109–1118.

Mott K.A. (1988) Do stomata respond to CO_2 concentrations other than intercellular. *Plant Physiology* **86,** 200–203.

Mott K.A. & Franks P.J. (2001) The role of epidermal turgor in stomatal interactions following a local perturbation in humidity. *Plant, Cell and Environment* **24,** 657–662.

Mott K.A. & Parkhurst D.F. (1991) Stomatal responses to humidity in air and helox. *Plant, Cell and Environment* **14,** 509–515.

Netting A.G. (2000) pH, abscisic acid and the integration of metabolism in plants under stressed and non-stressed conditions: cellular responses to stress and their implication for plant water relations. *Journal of Experimental Botany* **51,** 147–158.

Norman J.M., Kustas W.P. & Humes K.S. (1995) Source approach for estimating soil and vegetation energy fluxes in observations of directional radiometric surface temperature. *Agricultural and Forest Meteorology* **77,** 263–293.

Olioso A., Carlson T.N. & Brisson N. (1996) Simulation of diurnal transpiration and photosynthseis of a water stressed soybean crop. *Agricultural and Forest Meteorology* **81,** 41–59.

Pereira J.S., Tenhunen J.D. & Lange O.L. (1987) Stomatal control of photosynthesis of *Eucalyptus globulus* Labill. trees under field conditions in Portugal. *Journal of Experimental Botany* **38,** 1678–1688.

Perrier A. & Tuzet A. (1998) Approche Théorique Du Continuum Sol-Plante-Atmosphère. In *Traité d'irrigation* (ed. J.R. Tiercelin) Chap. II.4, pp. 112–146. Lavoisier, Paris, France.

Philip J.R. (1957) Evaporation, and moisture and heat fields in the soil. *Journal of Meteorology* **14,** 354–366.
Prior L.D., Eamus D. & Duff G.A. (1997) Seasonal and diurnal patterns of carbon assimilation, stomatal conductance and leaf water potential in *Eucalyptus tetrodonta* saplings in a wet-dry savanna in Northern Australia. *Australian Journal of Botany* **45,** 241–258.
Reid J.B. & Huck M.G. (1990) Diurnal variation of crop hydraulic resistance: a new analysis. *Agronomy Journal* **82,** 827–834.
Ronda R.J., de Bruin H.A.R. & Holtslag A.A.M. (2001) Representation of the canopy conductance in modelling the surface energy budget for low vegetation. *Journal of Applied Meteorology* **40,** 1431–1444.
Saliendra N.Z., Sperry J.S. & Comstock J.P. (1995) Influence of leaf water status on stomatal response to humidity, hydraulic conductance, and soil drought in *Betula occidentalis*. *Planta* **196,** 357–366.
Schulze E.-D. & Hall A.E. (1982) Stomatal responses, water loss and CO_2 assimilation rates of plants in contrasting environments. In *Physiological Plant Ecology II Water Relations and Carbon Assimilation* (eds O.L. Lange, P.S. Nobel, C.B. Osmond, H. Ziegler), pp. 181–230. Springer-Verlag, Berlin, Germany.
Seginer I. (1971) Wind effect on the evaporation rate. *Journal of Applied Meteorology* **10,** 215–220.
Sellers P.J., Berry J.A., Collatz G.J., Field C.B. & Hall F.G. (1992) Canopy reflectance, photosynthesis and transpiration. III. A reanalysis using improved leaf models and a new canopy integration scheme. *Remote Sensing of Environment* **42,** 187–216.
Sellers P.J., Randall D.A., Collatz G.J., Berry J.A., Field C.B., Dazlich D.A., Zhang C., Collelo G.D. & Bounoua L. (1996) A revised land surface parameterization (SiB2) for atmospheric GCMs. Part 1. Model formulation. *Journal of Climate* **9,** 676–705.
Sifaoui M.S. & Perrier A. (1978) Caractérisation de l'évaporation profonde. *International Journal of Heat and Mass Transfer* **21,** 629–637.
Sperry J.S. (2000) Hydraulic constraints on plant gas exchange. *Agricultural and Forest Meteorology* **104,** 13–23.
Takagi K., Tsuboya T. & Takahashi H. (1998) Diurnal hystereses of stomatal and bulk surface conductances in ralation to water vapor pressure deficit in cool-temperate wetland. *Agricultural and Forest Meteorology* **91,** 177–191.
Tardieu F. & Davies W.J. (1993) Integration of hydraulic and chemical signalling in the control of stomatal conductance and water status of droughted plants. *Plant, Cell and Environment* **16,** 341–349.
Tardieu F. & Simonneau T. (1998) Variability among species of stomatal control under fluctuating soil water status and evaporative demand: Modelling isohydric and anisohydric behaviours. *Journal of Experimental Botany* **49,** 419–432.
Tyree M.T. & Sperry J.S. (1988) Do woody plants operate near the point of catastrophic xylem dysfunction caused by dynamic water stress? Answers from a model. *Plant Physiology* **88,** 574–580.
Wang Y.P. & Leuning R. (1998) A two-leaf model for canopy conductance, photosynthesis and partitioning of available energy. I. Model description. *Agricultural and Forest Meteorology* **91,** 89–111.
Whitehead D., Walcroft A.S., Griffin K.L., Tissue D.T., Turnbull M.H., Engel V., Brown K.J. & Schuster W.S.F. (2002) Scaling carbon uptake from leaves to canopies: insights from two forests with contrasting properties. *Forests at the Land–Atmosphere Interface* (in press).
Williams M., Rastetter E.B., Fernandes D.N., Goulden M.L., Wofsy S.C., Shaver G.R., Melillo J.M., Munger J.W., Fan S.-M. & Nadelhoffer K.J. (1996) Modelling the soil-plant-atmosphere continuum in a *Quercus-Acer* stand at Harvard Forest: the regulation of stomatal conductance by light, nitrogen and soil/plant hydraulic conductance. *Plant, Cell and Environment* **19,** 911–927.
Wu H.-I., Sharpe J.H. & Spence R.D. (1985) Stomatal mechanics III: Geometric interpretation of the mechanical advantage. *Plant, Cell and Environment* **8,** 269–274.

Received 25 October 2002; received in revised form 17 January 2002; accepted for publication 24 January 2002

APPENDIX A

Models for canopy energy balance and CO_2 exchange.

Canopy energy balance

The conceptual structure of the canopy energy balance model is shown in Fig. 1. The model is a two-source (soil and vegetation) model of heat, water and carbon exchange between the canopy and the atmosphere (Choudhury & Monteith 1988; Norman, Kustas & Humes 1995; Anderson *et al*. 2000). Each flux from the canopy to the atmosphere (H, LE, F_{CO2}) consists of a contribution from the soil (subscript 's') and from the foliage layer (subscript 'v'). Here r_{bv} is the bulk boundary layer resistance, while r_{sH2O} and r_{sCO2} are the bulk stomatal resistances for H_2O and CO_2, respectively. The resistances R_s and R_v describe turbulent transport from the ground to the canopy source-sink height, h_s, and from h_s to the top of canopy (see Appendix c). An aerodynamic resistance r_a describe heat and mass (H_2O and CO_2) transport above the canopy (from the top of the canopy to a reference level, z_r). The foliage layer is characterized by a leaf surface temperature, T_{sv} (K) a bulk leaf water potential, Ψ_v (MPa) and a CO_2 concentration in the intercellular spaces, c_i (mol CO_2 mol^{-1} air). At h_s the characteristics of the air surrounding the leaves (temperature, T_{av}, vapour pressure, $P(T_{rv})$, and CO_2 concentration, c_v) result from turbulent transport through R_s and R_v. The soil surface is characterized by a surface temperature, T_{ss}.

The sensible heat fluxes from the soil surface H_s, the foliage layer H_v and the canopy (total flux) H are calculated, respectively, as:

$$H_s = \rho c_p \frac{T_{ss} - T_{av}}{R_s}$$
$$H_v = \rho c_p \frac{T_{sv} - T_{av}}{r_{bv}} \quad \text{(A1)}$$
$$H = H_s + H_v = \rho c_p \frac{T_{av} - T_a}{R_v + r_a}$$

where ρ is the air density, c_p is the specific heat of air at constant pressure, and T_a is the air temperature at the reference level, z_r, above the canopy.

Soil between the surface and the damping depth is divided into an upper, completely dry layer and a lower wet layer (Seginer 1971; Sifaoui & Perrier 1978; Choudhury & Monteith 1988). The damping depth d_s is related to the

thermal properties of the soil and the frequency of the temperature variation as follows:

$$d_s = \sqrt{\frac{2\lambda_w}{C_\omega}}$$

where λ_w is the thermal conductivity of wet layer, C is the volumetric heat capacity, ω equals 2π times the frequency of the temperature variation, thus for the diurnal variation $\omega = 2\pi/86\,400 = 7.27 \times 10^{-5}$ s^{-1}. Soil evaporation takes place at the top of the wet layer, at depth d_m, and the transfer of water vapour through the upper soil layer is regulated by a resistance r_m given by:

$$r_m = \frac{\xi d_m}{D_v f} \tag{A2}$$

where D_v is the water vapour diffusivity in air, f is the dry layer porosity and ξ is the tortuosity factor. As soil evaporation proceeds, the site of evaporation moves progressively deeper and the thickness of the dry layer changes according to$[\Delta d_m = E\Delta t/\theta_s]$, where E is the total evaporation flux density, Δt is the model time step, θ_s is the soil water content.

The latent heat fluxes from the soil surface LE_s, the foliage layer LE_v and the canopy LE are given by:

$$\begin{aligned} LE_s &= \frac{LM_v}{R}\frac{1}{R_s + r_m}\left(\frac{P(T_m)}{T_m} - \frac{P(T_{rv})}{T_{av}}\right) \\ LE_v &= \frac{LM_v}{R}\cdot\frac{1}{r_{sH2O} + r_{bv}}\left(\frac{h_i P(T_{sv})}{T_{sv}} - \frac{P(T_{rv})}{T_{av}}\right) \\ LE &= LE_s + LE_v = \frac{LM_v}{R}\frac{1}{R_v + r_a}\left(\frac{P(T_{rv})}{T_{av}} - \frac{P(T_r)}{T_a}\right) \end{aligned} \tag{A3}$$

where L is the latent heat of vaporization of water, M_v is the molecular weight of water vapour, R is the gas constant. Soil at the wet–dry interface is assumed to be saturated at a temperature, T_m and in the foliage elements, the vapour pressure of air in contact with the substomatal cavities is expressed as a function of the bulk leaf water potential, Ψ_v through $h_i = \exp(M_w J_v/\rho_v R T_{sv})$, the fractional relative humidity in the intercellular spaces.

Energy exchange between the canopy and the atmosphere satisfies the conservation equations:

$$\begin{aligned} Rn_v &= H_v + LE_v \\ Rn_s &= H_s + G_0 \\ G_0 &= LE_s + G_s \end{aligned} \tag{A4}$$

where Rn_v and Rn_s are the net absorption of radiation in the foliage layer and at the soil surface, respectively; and G_0 and G_s are the conduction downwards from the soil surface and into the wet soil layer, respectively. Partitioning of total net radiation between Rn_v and Rn_s is written as:

$$\begin{aligned} Rn_v &= (1-a_v)R_g(1-\exp(-k\cdot L_{AI})) + \\ &\quad \left(R_a - 2\sigma T_{sv}^4 + \varepsilon\sigma T_{ss}^4\right)(1-\exp(-k\cdot L_{AI})) \\ Rn_s &= (1-a_v)R_g\exp(-k\cdot L_{AI}) + \\ &\quad R_a\exp(-k\cdot L_{AI}) + \sigma T_{sv}^4(1-\exp(-k\cdot L_{AI})) \\ &\quad - \varepsilon\sigma T_{ss}^4 \end{aligned} \tag{A5}$$

where R_g is the global solar radiation above the canopy, a_v is the average canopy albedo, R_a is the long-wave radiation of the atmosphere, k is the extinction coefficient ($k = 0.7$) and L_{AI} is the leaf area index of the foliage. Soil heat fluxes G_0 and G_s are calculated by assuming linear temperature gradients:

$$\begin{aligned} G_0 &= \lambda_d \frac{T_{ss} - T_m}{d_m} \\ G_0 &= \lambda_w \frac{T_m - T_d}{d_d - d_m} \end{aligned} \tag{A6}$$

where λ_d is the thermal conductivity of the dry layer extending from the surface to d_m, T_m is the soil temperature at the dry–wet layer interface and T_d is the temperature at the damping depth d_d.

Canopy CO_2 exchange model

The CO_2 flux between the reference height and the canopy air space, F_{CO2}, arises as the effect of net canopy photosynthesis, A (positive toward the canopy in units of mol m^{-2} s^{-1}) and soil respiration, F_{soil} (positive upwards):

$$F_{CO2} = A - F_{soil} \tag{A7}$$

The net canopy photosynthesis, A is calculated using the detailed biochemical model of photosynthesis of Farquhar (Farquhar, von Caemmerer & Berry 1980) which is widely employed in both leaf and canopy-scale gas studies (Harley *et al*. 1992; Leuning *et al*. 1995; Sellers *et al*. 1996; Baldocchi & Meyers 1998; Wang & Leuning 1998). In this model CO_2 uptake is either limited by Rubisco activity and the respective partial pressures of the competing gases CO_2 and O_2 at the sites of carboxylation V_c or by electron transport, V_j which limits the rate at which Ribulose bisPhosphate (RuBP) is regenerated. Net canopy photosynthesis A may then be expressed as:

$$A = \min(V_c, V_j) - R_d \tag{A8}$$

where R_d is the rate of CO_2 evolution from processes other than photorespiration. The term $\min(V_c, V_j)$ represents the minimum of V_c and V_j. The assimilation rate, V_c, is given by:

$$V_c = V_{lmax}\frac{c_i - \Gamma_*}{c_i + K_c(1 + o_i/K_o)} \tag{A9}$$

where V_{lmax} is the maximum carboxylation rate per unit leaf area when RuBP is saturated, Γ_* is the CO_2 compensation point in the absence of day respiration, o_i is the intercellular oxygen concentration, and K_c and K_o are Michaelis coefficients for CO_2 and O_2, respectively. The rate of carboxylation limited solely by the rate of RuBP regeneration due to electron transport is calculated as:

$$V_j = \frac{J}{4}\frac{c_i - \Gamma_*}{c_i + 2\Gamma_*} \tag{A10}$$

where J is the electron transport rate for a given absorbed photon irradiance. Both V_c and V_j are functions of c_i and temperature, and V_j also depends on absorbed radiation.

Respiration is also dependent on leaf temperature. Parameter values and their dependence on leaf temperature are from Leuning (1995) and are summarized in Appendix B.

The maximum canopy photosynthetic capacity, V_{cmax} is calculated by an integral of the leaf photosynthetic capacity and the leaf nitrogen profile over the entire canopy (De Pury & Farquhar 1997):

$$V_{cmax} = L_{AI} V_{lmax} \frac{1-\exp(-k_n)}{k_n} \quad \text{(A11)}$$

where V_{lmax} is the maximum photosynthetic capacity per unit leaf area, L_{AI} is the leaf canopy area index and k_n is the coefficient of leaf nitrogen allocation.

The CO_2 flux, from the soil surface, F_{soil}, is computed using the Arrhenius equation:

$$F_{soil} = F_{0,soil} \exp(E_{a,soil}(T_{s10} - T_0)/RT_{s10}T_0) \quad \text{(A12)}$$

where $F_{0,soil}$ is the CO_2 flux from the soil at $T_0 = 298$ K ($F_{0,soil} = 3$ μmol m^{-2} s^{-1}), $E_{a,soil}$ is the activation energy ($E_{a,soil} = 53000$ J mol^{-1}), R is the universal gas constant, T_{s10} (K) is soil temperature at 10 cm. In this model T_{s10} is replaced with the soil temperature at the dry–wet layer interface T_m.

Canopy photosynthesis, A and net CO_2 flux from the canopy plus soil, F_{CO2}, are also governed by the biophysical control of canopy resistances and they are parameterized, respectively, as:

$$A = \frac{c_v - c_i}{\mu r_{bv}/\beta + 1/g_{CO2}}$$
$$F_{CO2} = A - F_{soil} = \frac{c_a - c_v}{(R_v + r_a)/\beta} \quad \text{(A13)}$$

where μ is the ratio of diffusivity of CO_2 and H_2O appropriate to leaf boundary layer diffusion and β (= P/RT) is the coefficient used to convert the molar units (mol^{-1} m^2 s) into physical resistance units (s m^{-1}) and P is the atmospheric pressure.

APPENDIX B

Parameters in the biochemical model of photosynthesis

The dependence of electron transport rate J on absorbed photon irradiance Q was modelled by Farquhar & Wong (1984) using the non-rectangular hyperbolic function:

$$\theta J^2 - (\alpha Q + J_{lmax})J + \alpha Q J_{lmax} = 0 \quad \text{(B1)}$$

where θ determines the shape of the non-rectangular hyperbola, J_{lmax} is the potential rate of whole-chain electron transport per unit leaf area and α is the quantum yield of whole-chain electron transport. Parameters values used in the photosynthesis model are given in Table 3.

The temperature sensitivity of the Michaelis–Menten constants K_c and K_o, the maximum photosynthetic capacity per unit leaf area V_{lmax} and the CO_2 compensation point in the absence of day respiration Γ_* were calculated following Leuning (1995). A normalized Arrhenius equation was used to represent the temperature dependence of K_c and K_o:

$$K_x = K_{x,ref} \exp\left(\frac{E_x}{RT_{ref}}\left(1 - \frac{T_{ref}}{T}\right)\right) \quad \text{(B2)}$$

in which R is the universal gas constant, E_x is the activation energy for K_x, where the subscript x stands for either c or o, and $K_{x,ref}$ is the value of K_x at a reference temperature T_{ref}.

The temperature function used for V_{lmax} is:

Table 3. Values of parameters used in the model of photosynthesis presented in Appendix B

Symbol	Parameter	Value	Units
T_{ref}	reference temperature	293.2	K
V_{lmax}^{ref}	max photosynthetic capacity at T_{ref}	100×10^6	mol CO_2 m^{-2} s^{-1}
$r_{0,soil}$	CO_2 flux from the soil at 298 K	3	μmol CO_2 m^{-2} s^{-1}
$E_{a,soil}$	activation energy for soil CO_2	53000	J mol^{-1}
o_i	intercellular oxygen concentration	210×10^{-3}	mol mol^{-1}
$K_{o,ref}$	Michaelis coefficient for O_2	256×10^{-3}	mol mol^{-1}
$K_{c,ref}$	Michaelis coefficient for CO_2	302×10^{-6}	mol mol^{-1}
E_o	activation energy for K_o	36 000.	J mol^{-1}
E_c	activation energy for K_c	59 430.	J mol^{-1}
E_{aV}	activation energy for V_{cmax}	58 520.	J mol^{-1}
E_{dV}	deactivation energy for V_{cmax}	220 000.	J mol^{-1}
E_{aJ}	activation energy for J_{max}	37 000.	J mol^{-1}
E_{dJ}	deactivation energy for J_{max}	220 000.	J mol^{-1}
S	entropy term for J_{max} and V_{cmax}	700.	J mol^{-1} K^{-1}
α	quantum yield	0.2	
θ	parameter of the hyperbola	0.9	
γ_0	parameter in Γ_* Eqn B4	28×10^{-6}	mol mol^{-1}
γ_1	parameter in Γ_* Eqn B4	0.0509	
γ_2	parameter in Γ_* Eqn B4	0.0010	

$$V_{\mathrm{lmax}}\frac{V_{\mathrm{lmax}}^{\mathrm{ref}}\exp((E_{\mathrm{a}}/\mathrm{RT}_{\mathrm{ref}})(1-T_{\mathrm{ref}}/T))}{1+\exp((ST-E_{\mathrm{d}})/RT)} \quad \text{(B3)}$$

where $V_{\mathrm{lmax}}^{\mathrm{ref}}$ is the value of V_{lmax} at T_{ref}, E_{a} is the energy of activation, E_{d} is the energy of de-activation and S is an entropy term. The potential rate of electron transport per unit leaf area at the reference temperature $J_{\mathrm{lmax}}^{\mathrm{ref}}$ is assumed to be proportional to $V_{\mathrm{lmax}}^{\mathrm{ref}}$ and the proportionality coefficient is equal to 2.0 (Leuning 1997).

A second-order polynomial was used to describe the temperature dependence of Γ_*, namely

$$\Gamma_* = \gamma_0\left(1+\gamma_1(T-T_{\mathrm{ref}})+\gamma_2(T-T_{\mathrm{ref}})^2\right) \quad \text{(B4)}$$

where γ_0, γ_1, and γ_2 are empirical coefficients, T is leaf temperature and T_{ref} is a reference temperature.

APPENDIX C

Aerodynamic resistances

The aerodynamic resistances R_{s}, R_{v} and r_{a} (Fig. 1) are calculated assuming an exponential profile of wind speed $u(z)$ and eddy diffusivity $K(z)$ inside the canopy:

$$u(z)=u(h_{\mathrm{c}})\exp\left(\eta\left(\frac{z}{h_{\mathrm{c}}}-1\right)\right)$$
$$K(z)=K(h_{\mathrm{c}})\exp\left(\eta\left(\frac{z}{h_{\mathrm{c}}}-1\right)\right) \quad \text{(C1)}$$

where $u(h_{\mathrm{c}})$ and $K(h_{\mathrm{c}})$ are the wind speed and eddy diffusity at the canopy top, respectively, and η is the extinction factor. Assuming a vertically homogeneous canopy with a constant mixing length l_{c}, η is expressed as:

$$\eta = h_{\mathrm{c}}\left(\frac{c_{\mathrm{d}}L_{\mathrm{AI}}/h_{\mathrm{c}}}{2l_{\mathrm{c}}^2}\right)^{1/3} \quad \text{(C2)}$$

where c_{d} is the leaf drag coefficient (Inoue 1963). Thus, R_{s} and R_{v} and r_{a} are obtained using:

$$R_{\mathrm{s}}=\int_{z_{0\mathrm{g}}}^{h_{\mathrm{s}}}\frac{dz}{K(z)};\quad R_{\mathrm{v}}=\int_{h_{\mathrm{s}}}^{h_{\mathrm{c}}}\frac{dz}{K(z)};\quad r_{\mathrm{a}}=\int_{h_{\mathrm{c}}}^{z_{\mathrm{r}}}\frac{dz}{K(z)} \quad \text{(C3)}$$

where $z_{0\mathrm{g}}$ is the roughness length of soil surface.

Finally, the bulk boundary layer resistance r_{bv} can be written as:

$$\frac{1}{r_{\mathrm{bv}}}=\frac{1}{h_{\mathrm{c}}-z_{0\mathrm{g}}}\int_{z_{0\mathrm{g}}}^{h_{\mathrm{c}}}\frac{u(h_{\mathrm{c}})^{0.5}}{C_t d_{\mathrm{l}}^{0.5}}\exp\left(\frac{\eta}{2}\left(\frac{z}{h_{\mathrm{c}}}-1\right)\right) \quad \text{(C4)}$$

where d_{l} is the average leaf width and C_{t} is the transfer coefficient ($C_{\mathrm{t}}=156.2$).

APPENDIX D

List of variables, categorized by the models in which they are used

Symbol	Units	Description
Canopy energy balance model		
C	J m^{-3} K^{-1}	soil volumetric heat capacity
c_{d}	–	leaf drag coefficient
c_{p}	J kg^{-1} K^{-1}	specific heat of air at constant pressure
d_{d}	m	damping depth of the thermal wave
d_{l}	m	average leaf width
d_{m}	m	thickness of the upper dry soil layer
D_{v}	m^2 s^{-1}	water vapour diffusivity in air
f	–	dry layer porosity
G_0	W m^{-2}	conduction downwards from the soil surface
G_{s}	W m^{-2}	conduction into the wet soil layer
H	W m^{-2}	sensible heat flux from the canopy (total flux)
h_{c}	m	height of the canopy
h_{s}	m	canopy source-sink height
H_{s}	W m^{-2}	sensible heat flux from the soil surface
H_{v}	W m^{-2}	sensible heat flux from the foliage layer
k	–	extinction coefficient of radiation
K(z)	m^2 s^{-1}	eddy diffusivity at level z
L	J kg^{-1}	latent heat of vaporization of water
L_{AI}	–	leaf area index of the foliage
l_{c}	m	canopy mixing length
LE	W m^{-2}	latent heat fluxes from the canopy
LE_{s}	W m^{-2}	latent heat fluxes from the soil surface
LE_{v}	W m^{-2}	latent heat fluxes from the foliage layer
M_{v}	kg mol^{-1}	molecular weight of water vapour
P	MPa	atmospheric pressure

APPENDIX D (*Continued*)

Symbol	Units	Description
$P(T)$	MPa	saturation water vapour pressure at temperature T
R	J K^{-1} mol^{-1}	ideal gas constant
r_a	s m^{-1}	aerodynamic resistance for heat and mass above the canopy
R_a	W m^{-2}	long-wave radiation of the atmosphere
r_{bv}	m s^{-1}	bulk boundary layer resistance
R_g	W m^{-2}	global solar radiation above the canopy
r_m	s m^{-1}	resistance to water vapour transfer through the dry soil layer
Rn	W m^{-2}	net absorption of radiation in the canopy
Rn_s	W m^{-2}	net absorption of radiation at the soil surface
Rn_v	W m^{-2}	net absorption of radiation in the foliage layer
R_s	s m^{-1}	turbulent transport resistance from the ground to h_s
r_{sCO2}	s m^{-1}	bulk stomatal resistance for CO_2
r_{sH2O}	s m^{-1}	bulk stomatal resistance for H_2O
R_v	s m^{-1}	turbulent transport resistance from h_s to the top of canopy
T_a	K	air temperature at the reference level, z_r
T_{av}	K	temperature of the air surrounding leaves
T_d	K	temperature at the damping depth
T_m	K	soil temperature at the dry–wet layer interface
T_r	K	dew point temperature at the reference level, z_r
T_{rv}	K	dew point temperature of the air surrounding leaves
T_{ss}.	K	soil surface temperature
T_{sv}	K	foliage temperature
$u(z)$	m s^{-1}	wind speed at level z
z_{0g}	m	roughness length of soil surface
z_r	m	reference level above the canopy
a_v	–	average canopy albedo
ξ	–	dry layer tortuosity factor
ω	s^{-1}	2π times the frequency of the temperature variation
λ_d	W m^{-1} K^{-1}	thermal conductivity of the of the upper dry soil layer
λ_w	W m^{-1} K^{-1}	thermal conductivity of the wet layer
η	–	extinction factor of wind
ρ	kg m^{-3}	air density
Δt	s	model time step
Stomatal conductance model		
a	–	empirical coefficient
$f_{\psi v}$	–	empirical function (sensitivity of stomata to leaf water potential)
g_0	mol m^{-2} s^{-1}	limiting value of g_{CO2} at the light compensation point
g_{CO2}	mol m^{-2} s^{-1}	stomatal conductance for CO_2
s_f	MPa^{-1}	sensitivity parameter
Γ	mol mol^{-1}	CO_2 compensation point
ψ_f	MPa	reference potential
ψ_v	MPa	leaf water potential
Plant water transfer model		
b	–	empirical parameter
F	m^3 m^{-2} s^{-1}	flow of water through the plant canopy
h_i	–	relative humidity in the intercellular spaces
K_s	s^{-1} MPa^{-1} m^2	soil hydraulic conductivity
K_{sat}	s^{-1} m^2	matric flux potential
L_r	m m^{-3}	root length per soil volume
r	m	soil radial distance from the axis of the root
t	s	time of day
z_{root}	m	root depth
ψ_e	MPa	air entry water potential of the soil
ψ_r	MPa	water potential of the roots
θ_s	m^3 m^{-3}	soil water content
Ψ_s	MPa	soil water potential
θ_{sat}	m^3 m^{-3}	saturation water content of the soil
ρ_v	kg m^{-3}	liquid water density
χ_v	MPa s m^{-1}	plant hydraulic resistance
Canopy CO_2 exchange model		
$F_{0,soil}$	mol m^{-2} s^{-1}	CO_2 flux from the soil at $T_0 = 298$ K
V_{lmax}^{ref}	mol m^{-2} s^{-1}	max carboxylation rate per unit leaf area at T_{ref}

APPENDIX D (*Continued*)

Symbol	Units	Description
A	mol m^{-2} s^{-1}	net canopy photosynthesis
c_i	mol mol^{-1}	CO_2 concentration in the intercellular spaces
$E_{a,soil}$	J mol^{-1}	soil activation energy
E_{aJ}	J mol^{-1}	activation energy for J_{max}
E_{aV}	J mol^{-1}	activation energy for V_{cmax}
E_c	J mol^{-1}	activation energy for K_c
E_{dJ}	J mol^{-1}	deactivation energy for J_{max}
E_{dV}	J mol^{-1}	deactivation energy for V_{cmax}
E_o	J mol^{-1}	activation energy for K_o
F_{CO2}	mol m^{-2} s^{-1}	CO_2 flux between the reference height and the canopy air space
F_{soil}	mol m^{-2} s^{-1}	CO_2 flux, from the soil surface
J	mol m^{-2} s^{-1}	electron transport rate for a given absorbed photon irradiance
V_{lmax}	mol m^{-2} s^{-1}	maximum carboxylation rate per unit leaf area
K_c	mol mol^{-1}	Michaelis coefficient for CO_2
$K_{c,ref}$	mol mol^{-1}	Michaelis coefficient for CO_2 at T_{ref}
k_n	–	coefficient of leaf nitrogen allocation
K_o	mol mol^{-1}	Michaelis coefficient for O_2
$K_{o,ref}$	mol mol^{-1}	Michaelis coefficient for O_2 at T_{ref}
o_i	mol mol^{-1}	intercellular oxygen concentration
S	J mol^{-1} K^{-1}	entropy term for J_{max} and V_{cmax}
T_{ref}	K	reference temperature
T_{s10}	K	soil temperature at 10 cm
V_c	mol m^{-2} s^{-1}	Rubisco activity at the sites of carboxylation
V_j	mol m^{-2} s^{-1}	electron transport
α	–	quantum yield
μ	–	ratio of diffusivities appropriate to leaf boundary layer diffusion
β	mol m^{-3}	coefficient to convert molar units into physical resistance units
θ	–	parameter of the hyperbola
Γ_*	mol mol^{-1}	CO_2 compensation point in the absence of day respiration
γ_0	mol mol^{-1}	parameter in Γ_* equation
γ_1	–	parameter in Γ_* equation
γ_2	–	parameter in Γ_* equation